HHS Public Access

Author manuscript

Dev Dyn. Author manuscript; available in PMC 2019 June 01.

Published in final edited form as:

Dev Dyn. 2018 June ; 247(6): 832–853. doi:10.1002/dvdy.24630.

Evolution of caudal fin ray development and caudal fin hypural diastema complex in spotted gar, teleosts, and other neopterygian fishes

Thomas Desvignes[*], **Andrew Carey**, and **John H. Postlethwait**

Institute of Neuroscience, University of Oregon, Eugene OR 97403, USA

Abstract

Background—The caudal fin of actinopterygians transitioned from a heterocercal dorsoventrally asymmetrical fin to a homocercal externally symmetrical fin in teleosts through poorly understood evolutionary developmental mechanisms. We studied the caudal skeleton of major living actinopterygian lineages, including polypteriformes, acipenseriformes, Holostei (gars and bowfin), and teleosts, compared to reports of extinct neopterygians and basal teleosteans. We focused on the hypural diastema complex, which includes 1) a gap between hypurals 2 and 3, that 2) separates two plates of connective tissue at 3) the branching of caudal vasculature; these features had been considered as a shared, derived trait of teleosts, a synapomorphy.

Results—These studies revealed that gars and teleosts share all three features of the hypural diastema complex. Absence of a complex with these features from bowfin, fossil Holostei, and stem Teleostei argues in favor of repetitive, independent emergence in several neopterygian and basal Teleostei lineages, or less likely, many independent losses. We further observed that in gars and teleosts, the earliest developing lepidotrichia align with the horizontal adult body axis, thus participating in external symmetry.

Conclusions—These results suggest that the hypural diastema complex in teleosts and gars represents a homoplasy among neopterygians and that it emerged repeatedly by parallel evolution due to shared inherited underlying genetic and developmental programs (latent homology). Because the hypural diastema complex exists in gars with heterocercal tails, this complex is independent of homocercality.

Keywords

Ontogeny; plate of connective tissue; Lepisosteus; Amia calva; Holostei; Danio rerio; Gasterosteus aculeatus; tail

[*]Corresponding author: Thomas Desvignes, Ph.D., Institute of Neuroscience, University of Oregon, 1254 University of Oregon, 222 Huestis Hall, Eugene, OR 97403, Phone: 541-346-4556, desvignes@uoneuro.uoregon.edu.

Authors' contributions

Study concept and design: T.D., and J.H.P. Acquisition of data: T.D., and A.C. Analysis and interpretation of data: T.D., A.C., and J.H.P. Drafting of the manuscript: T.D., A.C., and J.H.P. Critical revision of the manuscript: T.D., A.C, and J.H.P. Obtained funding: J.H.P. Study supervision: T.D. and J.H.P.

Introduction

The actinopterygii (ray-finned fishes), is the most species-rich group of vertebrates, including over 32,000 living species, about half of all extant vertebrates (Nelson, 2006; Faircloth et al., 2013; Sallan, 2014; Eschmeyer, 2015). A major innovation in ray-finned fish evolution involved enhanced locomotion control enabled by changes in the morphology of the dorsal and anal fins in neopterygian fishes (meaning “fish with new fins”). The evolution of dorsal and anal fins in which each basal skeletal element associates with just one long distal radial element occurred along with other morphological innovations, for example in the skull and mouth, that improved prey capture. Together, these suites of characters provided advantages that allowed neopterygians to become the taxonomically dominant group of vertebrates (López-Arbarello, 2012).

Among neopterygians, the largely dominant Teleostei infraclass, representing more than 99.9% of living actinopterygian species (Nelson, 2006; Eschmeyer, 2015), possesses both genomic and morphological innovations. Genomically, a whole genome duplication event, the Teleost Genome Duplication (TGD), provided teleosts with two copies of every ancestral gene, only about a quarter of which survive in duplicate in modern teleosts (Amores et al., 1998; Postlethwait et al., 1998; Taylor et al., 2003; Jaillon et al., 2004). Morphologically, numerous teleost-specific characteristics evolved, including additional innovations in the jaw and the emergence of a homocercal caudal fin that tends to be externally symmetrical dorsoventrally (Schultze and Arratia, 1989, 2013; Sallan, 2014; Arratia, 2015). Genomic and morphological innovations may both have contributed to the success of teleosts. Indeed, the caudal fin is a major component of mobility in fishes because it generates swimming power and contributes to maneuverability, thus improving control of swimming speed, agility, prey capture, and predator avoidance (Lauder, 2000; Flammang and Lauder, 2009). The caudal fin and its skeleton are highly variable among species according to species history and environment, and thus contribute to ecological, biomechanical, and systematic studies (eg. (Grünbaum et al.; Schultze and Arratia, 1986, 1988, 2013; Arratia and Schultze, 1992; Lauder, 2000; Cloutier and Arratia, 2004; Flammang and Lauder, 2009; Cloutier et al., 2011; Fiaz et al., 2012)).

While homocercality is often mistakenly associated solely with caudal fin dorsoventral symmetry, the key feature is actually characterized by a notochord that ends shortly beyond the posterior margin of the most posterior skeletal element rather than extending along the dorsal margin of the first principal caudal-fin ray as in heterocercal caudal fins (Arratia, 2015). Living teleosts have a homocercal caudal fin composed of one or two lobes that generally appear from the outside to have dorsoventral symmetry. In contrast, most non-teleost ray-finned fishes have a heterocercal caudal fin, which corresponds to the ancestral character state, predating the divergence of ray-finned fishes and lobe-finned fishes; the heterocercal caudal fin can appear externally to be either symmetrical or asymmetrical (Schultze and Arratia, 1989; Metscher and Ahlberg, 2001; Moriyama and Takeda, 2013). For example, among Neopterygians, the Holostei, which includes gars and bowfin as the only living representatives, is the sister group to the teleosts (Nelson, 2006; Faircloth et al., 2013; Sallan, 2014; Eschmeyer, 2015) although holosteans possess a seemingly symmetrical caudal fin formed by a single caudal fin lobe, their caudal fin is nonetheless heterocercal

because the notochord extends to the posterior tip of the fin on the dorsal side of the most dorsal ray.

The sister group of the Neopterygii, the acipenseriformes (sturgeons and paddlefish), also have a heterocercal caudal fin that is asymmetrical because it is formed by two unequal dorsal and ventral lobes, and in which the notochord extends to the tip of the dorsal lobe (Grande and Bemis, 1991; Bemis and Grande, 1999; Metscher and Ahlberg, 2001; Hilton, 2004). The most basal living ray-finned fishes, the polypteriformes, which includes bichirs and reedfish, constitute the sister group of the Neopterygii + Acipenseriformes. Polypteriformes have a secondarily derived, roughly symmetrical caudal fin, called diphycercal, in which the vertebral column extends to the tip of the fin (Bartsch and Gemballa, 1992; Metscher and Ahlberg, 2001; Moriyama and Takeda, 2013).

Although the teleost homocercal caudal fin usually appears externally to be a symmetrical fin with equal upper and lower lobes, the internal organization of the teleost caudal skeleton is highly asymmetrical (e.g. (Schultze and Arratia, 1989; Metscher and Ahlberg, 2001; Moriyama and Takeda, 2013)). Indeed, Huxley described the teleost homocercal caudal fin long ago as “excessively heterocercal” (Huxley, 1859) after finding that the symmetrical adult stickleback caudal skeleton doesn’t arise from dorsoventrally symmetrical skeletal elements, but instead develops from dramatic modifications of the vertebral column on which ventral skeletal elements bend upwards and support an exteriorly symmetrical caudal fin. Despite numerous studies on caudal fin skeletons, the process by which the caudal fin transitioned from a heterocercal morphology in neopterygians to a homocercal form in teleosts is still not well understood. This lack of understanding is due partly to the facts that: 1) understanding skeletal evolution relies mostly on fully mineralized fossil skeletons of adult individuals; 2) in fossils, some elements may not be intact or visible (covered by scales for example); 3) evolutionary intermediates or novel lineages are rare and often difficult to classify with respect to other described lineages; and 4) only 49 species of non-teleost actinopterygians remain extant (12 species of polypteriformes, 29 species of acipenseriformes, and 8 species of holostei) from the rich diversity of ray-finned fishes that existed between the emergence of actinopterygians about 400 million years ago (mya) and the appearance of teleosts about 330–270 mya (Near et al., 2012; Sallan, 2014; Arratia, 2015); this paucity of surviving lineages limits the range of species available for the analyses of different developmental stages that provide insight into character origins. Indeed, the rarity of young non-mineralized or partially mineralized developmental stages in fossils limits the study of skeletal ontogeny that could, in principle, reveal vestigial or transitory characters that are not apparent in adults (Hall, 2003; Wanninger, 2015). Detailed comparative analyses of development in non-teleost and teleost actinopterygians are thus necessary to better understand the developmental evolutionary mechanisms that gave rise to the homocercal caudal fin.

Here, we analyzed, in a phylogenetic context, newly described caudal fin skeletal features among gars (Lepisosteiformes) (Desvignes et al., 2018) and their potential role in the establishment of symmetry in neopterygians and homocercality in teleosts. More specifically, we focused attention on previously undescribed endoskeletal and mesodermal features associated with hypurals 2 and 3, recalling the hypural diastema in teleosts (Arratia,

2013; Schultze and Arratia, 2013) by including a consistent gap between two adjacent hypurals that separates a pair of plates of connective tissue, and dermoskeletal features like the earliest-forming pair of caudal lepidotrichia, which we find to develop at hypurals 1 and 2 in contrast to previous description at hypurals 2 and 3 (Metscher and Ahlberg, 2001) (Desvignes et al., 2018). We analyzed the evolution of these features by applying concepts from morphology, developmental biology, evolutionary biology, and phylogenetics, and by combining observations of spotted gar with detailed analyses of the caudal skeleton of other major living actinopterygian lineages, including polypteriformes (grey bichir *Polypterus senegalus*), acipenseriformes (American paddlefish *Polyodon spathula*), holostei (bowfin *Amia calva*) and teleosts (zebrafish *Danio rerio* and three-spined stickleback *Gasterosteus aculeatus*, henceforth simply stickleback), as well as extinct neopterygian and basal teleostean lineages based on published literature. This analysis helps us to understand the organization and evolutionary relationships of some previously undocumented skeletal elements and developmental features in actinopterygians and to interpret the succession of character states that led to the establishment of homocercality in teleosts from heterocercality in ancestral neopterygians.

Results

This Results section describes in detail the development of the caudal fin of each species, including some structures not directly relevant to the main discussion, for readers interested in all aspects of caudal fin morphology and development.

Bichir

Our description of caudal fin evolution among ray-finned fishes begins with the polypteriformes, the most basally diverging lineage (Fig. 1A). Polypteriformes (bichirs and reedfish) possess a secondarily derived, externally symmetrical diphycercal caudal fin with several notable characteristics, including the inclusion of pterygiophores originating from the dorsal fin; this organization differs significantly both from other actinopterygians and from the ancestral heterocercal caudal fin shape (Bartsch, 1988; Metscher and Ahlberg, 2001; Cloutier and Arratia, 2004; Moriyama and Takeda, 2013). The secondarily derived diphycercal caudal fin in polypteriformes thus limits the usefulness of bichirs in understanding the evolution of actinopterygian caudal fins. Our adult specimen (*Polypterus senegalus*, 161 mm TL) had a straight vertebral column that terminated in a cartilaginous element pointing slightly into the upper lobe after the last ural centrum, ural centrum 5 (Fig. 1L insert, u5), confirming a previous report (Bartsch and Gemballa, 1992). The caudal fin skeleton contained ventrally five evenly spaced hypurals and five haemal spines supporting the ventral caudal fin rays (Fig. 1L, cfr), in agreement with a previous report of five to six hypurals in bichirs (Bartsch and Gemballa, 1992) and an illustration depicting five hypurals and five haemal spines (Komagata et al., 1993).

Our grey bichir lacked ventral distal caudal radials associated with either hypurals or haemal spines, confirming previous observations (Bartsch and Gemballa, 1992). Dorsally, all preural centra and ural centrum 1 each held a supraneural (sn) that was not fused to the centrum (i.e. autogenous), a median, elongated rod-like skeletal element developing independently from

the neural spine or neural arch (Fig. 1L). In contrast, ural centra 2 to 5 lacked supraneurals (Fig. 1L, insert) and lacked epurals and neural spines, as in previous descriptions (Bartsch and Gemballa, 1992). Six caudal pterygiophores, independent of the axial skeleton, were intercalated dorsally between supraneurals (Fig. 1L). Rather than including these six pterygiophores as a part of the dorsal fin (Bartsch and Gemballa, 1992), we prefer to include them as caudal pterygiophores due to their direct incorporation into the caudal fin lobe, whereas the more anterior dorsal pterygiophores are individualized and the rays they associate with are gathered into finlets or pinnulae (Fig. 1L). The anterior-most three ural centra and neural arches were fully mineralized, while ural centra 4 and 5 were partially mineralized (Fig. 1L). Ural vertebra 4 had the neural arch and the dorsal half of the centrum mineralized and ural vertebra 5 had only the roof of the neural arch mineralized (Fig. 1L). Ventrally, the ural centra showed a small zone of mineralization close to the hypural articulation on ural centra 3 and 4 (Fig. 1L, varc). This mineralization pattern suggests that this bichir's centra mineralized mainly from the dorsal arcualia and only marginally from ventral arcualia. In our specimen, hypural 1 (Fig. 1L, white triangle) articulated both with preural centrum 1 anteriorly and ural centrum 1 posteriorly (Fig. 1L). Likewise, hypurals 2 and 3 each articulated both with their corresponding centrum and the one just anterior to it (Fig. 1L). Finally, although the cartilaginous element terminating the vertebral column has been referred to as a urostyle (Bartsch, 1988; Bartsch and Gemballa, 1992), based on our specimen, this element seemed to be a compound cartilaginous element resulting from the fusion of the posterior neural arches. This element, located dorsally to the notochord similarly to bowfin's ural neural arch, differs from the opisthural cartilage which is located at the posterior tip of the notochord in some teleosts. We therefore prefer to refer to this element as a "ural neural arch" (Fig. 1L, una), as in bowfin (Nybelin, 1977; Schultze and Arratia, 1986; Grande and Bemis, 1998).

Paddlefish

The next diverging branch that survives on the actinopterygian tree (Fig. 1A) is the acipenseriformes, the largest extant group of non-teleost actinopterygian fishes (Hilton, 2004). As a representative of the acipenseriformes, we examined the American paddlefish (*Polyodon spathula*) using 14 young specimens ranging from 10 mm TL to 85 mm TL. The caudal skeleton began to develop hypaxially between 10 and 12 mm TL along with the initial upward flexion of the notochord around the putative first hypural (Fig. 2O, white triangle), as in another reported specimen (Bemis and Grande, 1999). At that stage, actinotrichia were present both ventral and dorsal to the notochord (Fig. 2O). In paddlefish larger than 51 mm TL, the vertebral column flexed into the upper lobe around hypural 1 (Fig. 1J, Fig. 2P–P′) and the caudal fin skeleton possessed about 20 to 30 individualized hypurals that became smaller posteriorly, followed by about ten small, rounded and incompletely individualized hypurals that appear partially fused to their neighboring hypurals (Fig. 2Q), as in previous observations of paddlefish (Grande and Bemis, 1991; Bemis and Grande, 1999; Arratia et al., 2001) and sturgeon (Bartsch, 1988). Hypural 1 was identified by a notch on the proximal end of the hypaxial element (Fig. 2P′, n-hyp1) according to previous work (Grande and Bemis, 1991; Bemis and Grande, 1999). In some of our specimens, as in samples reported by others, the notch at the base of the hypural 1 was

not always visible and therefore the precise identification of the first hypural in paddlefish was in question for some specimens.

Anterior to the hypurals, seven haemal elements were present (Fig. 1K, Fig. 2P–P′); likewise a published photograph and interpretive drawing of a 47 mm TL paddlefish had seven haemal spines (Bemis and Grande, 1999). Our 65 mm TL paddlefish lacked individualized basiventral arcualia (bv) which seemed to have already merged with the haemal spines forming the haemal arches; interventral arcualia (iv), however, were visible between hypural 1 and the parhypural (Fig. 2P′), and appeared in a larger specimen (85 mm TL) to have fused to the haemal arches. To our knowledge, the participation of the interventral arcualia in the formation of the ventral side of paddlefish vertebrae has not yet been reported, but is in agreement with similar observations made on another member of the acipenseriformes, the shortnose sturgeon *Acipenser brevirostrum* (Hilton et al., 2011).

In the paddlefish caudal fin, a row of block-like elements (bd) bordered the dorsal edge of the notochord from before the caudal peduncle to the tip of the fin (Fig. 1J, Fig. 2P′–Q). These elements saddling the notochord likely correspond to basidorsal arcualia that eventually form neural arches (Grande and Bemis, 1991; Bemis and Grande, 1999). In both the caudal peduncle and caudal fin, a second row of numerous and irregularly shaped cartilage elements were positioned just above the row of block-like elements and were present posteriorly until the tip of the caudal fin where both rows became less and less individualized (Fig. 2P′–Q). This upper row of Alcian-staining elements seems to be the continuation in the caudal fin of the supraneural series observed in the caudal region (Grande and Bemis, 1991; Bemis and Grande, 1999); we therefore call them “supraneurals of the caudal fin” (sncf).

Mineralization of paddlefish hypaxial elements began around 80 mm TL and appeared as a faint Alizarin Red stain at the distal half of the first haemal spines and the first few hypurals. In our samples, mineralization appeared to initiate in smaller animals than in samples in another study, in which hypurals were reported to remain unossified in a 125 mm TL individual (Grande and Bemis, 1991). Differences in staining protocols (non-acidic stain in our case, acidic stain in (Grande and Bemis, 1991)) could however be responsible for these differences.

Distal caudal radials (dcr), which formed triangular shaped blocks intercalated between hypaxial elements, were present near the distal epiphyses of hypurals 1 and 2 and the first five or six haemal spines, and occasionally at the distal tip of hypural 3 and more posterior (Fig. 1J, Fig. 2P′), as previously reported in paddlefish and sturgeon (Bartsch, 1988; Grande and Bemis, 1991; Bemis and Grande, 1999; Metscher and Ahlberg, 2001; Hilton, 2004). Numerous early developing and not yet mineralized caudal fin rays were present by 65 mm TL, from the caudal peduncle to the tip of the caudal fin (Fig. 1K, Fig. 2P′–Q). Based on our samples, we were unable to determine where the first lepidotrichia formed because our youngest individual (51 mm TL) already had many lepidotrichia, but Bemis and Grande (1999) depicted the earliest-forming lepidotrichia around hypural 2 in a 30 mm TL specimen, although the earliest lepidotrichia were proposed to be at the hypural/parhypural boundary by Metscher and Ahlberg (2001). Notably, no rays dorsal to the notochord were

present in any of our specimens. However, because epichordal lepidotrichia are known to be present in large acipenseriformes, in both sturgeons and paddlefish (Grande and Bemis, 1991; Hilton, 2004), they must form later in development than 85 mm TL, which is the most advanced stage we studied.

Our 85 mm TL paddlefish had nine developing dorsal fulcra and one ventral fulcrum that faintly stained with Alcian Blue but were not yet mineralized (Fig. 1J, Fig. 2P′–Q, fub), which is similar to our findings in spotted gar (Fig. 5L in (Desvignes et al., 2018)) and similar to *Elops affinis* (Arratia, 2009), a basally diverging living teleost (Elopiformes). The number of fulcra and their developmental timing was consistent with the report of five dorsal fulcra and one ventral fulcrum in a 47 mm TL long paddlefish (Bemis and Grande, 1999), ten dorsal and one ventral fulcrum in an 80 mm TL long paddlefish (Grande and Bemis, 1991) and multiple dorsal fulcra and one ventral fulcrum as a general case in acipenseriformes (Bartsch, 1988; Hilton, 2004).

Bowfin

Holosteans represent the surviving sister group of teleosts and include gars and bowfin (*Amia calva*), the extant sister group of the gars (Fig. 1A). We studied caudal skeletons from two juvenile bowfin of different sizes (34 mm and 99 mm TL, stained with Alcian Blue and Alizarin Red) and two adult specimens (181 mm and 233 mm TL, stained with Alizarin Red only). In the 34 mm TL juvenile bowfin, the notochord had already flexed slightly into the upper lobe around the first hypurals, signaling the beginning of a heterocercal caudal fin (Fig. 2M); the heterocercal nature of the caudal fin was well established in our 99 mm TL juvenile (Fig. 2N). Caudal fin skeletons of both juvenile bowfin had 11 hypurals ventrally that decreased progressively in size towards the posterior and had nine haemal spines supporting caudal fin rays (Fig. 2M″–N). At 34 mm TL, mineralization of bowfin hypurals and haemal elements was almost complete except at the distal parts of hypaxial elements, in the haemal arches, and in the two last hypurals (Fig. 2M″), in agreement with the previously described mineralization pattern (Grande and Bemis, 1998). At 99 mm TL, the haemal and neural arches were still cartilaginous while all hypurals were fully mineralized (Fig. 2N).

Centra had also started to mineralize in our 34 mm TL young bowfin. Abdominal and caudal centra appeared to be mineralizing in an anterior-posterior sequence, starting first around the basidorsal and interdorsal arcualia, followed by the basiventral and interventral arcualia (Fig. 2M′), as observed in a 26 mm SL bowfin (Grande and Bemis, 1998). Preural centra 3 to 1 and ural centra 1 to 3, began to mineralize ventrally, presumably from the basiventral autocentra enclosing the basiventral arcualia (Schultze and Arratia, 1986, 1989), before the anterior preural centra mineralized (Fig. 2M″), as reported (Grande and Bemis, 1998). At 99 mm TL, all abdominal centra and the first three ural centra were fully mineralized while ural centra 4 and 5 were only partially mineralized. In our larger juvenile and the two adult bowfin, abdominal centra and most caudal centra were diplospondylous (i.e. composed of two hemicentra) but preural centra 1 and 2 and all ural centra were monospondylous (i.e. composed of a single centrum) (Fig. 1H, Fig. 2N), as in previous reports (Schultze and Arratia, 1986, 1989; Grande and Bemis, 1998).

In our two adult bowfin, the caudal fin consisted of ten and 12 hypurals, nine and 11 haemal spines, four and eight mineralized ural centra, and a few partially mineralized posterior centra (Fig. 1H), as found in other studies (Nybelin, 1977; Schultze and Arratia, 1986, 1989; Grande and Bemis, 1998). All haemal arches and hypural 1 were autogenous whereas hypural 2 and posterior hypurals were fused at their proximal end with the centra (Fig. 1H), as in previous reports (Schultze and Arratia, 1986; Bartsch, 1988; Grande and Bemis, 1998). Notably, whereas one of our adult specimens retained a one-to-one relationship between ural centra and hypurals (Fig. 1H), the other showed fusions of ural centra, giving compound U2+3, U4+5+6 and U7+8 and a succession of a few partially mineralized rudimentary centra disconnected from the proximal ends of the hypurals (Data not shown). Similar fusion events for ural centra have previously been reported (Nybelin, 1977; Schultze and Arratia, 1986), but seem to be infrequent (Grande and Bemis, 1998). The absence of fusion between the last few hypurals and their respective rudimentary mineralized centra may be related mechanically to the upward flexion of the notochord, similarly to what was proposed in gars (Schultze and Arratia, 1986).

Dorsally, in the juvenile bowfin, all preural centra and ural centrum 1 had a cartilaginous neural arch bearing a median mineralizing neural spine (Fig. 2M″–N). Ural centrum 2 carried a small cartilaginous neural arch (Fig. 2M″), which was fully elongated by 99 mm TL (Fig. 2N), and more posterior centra displayed, in both juveniles, a “ural neural arch”, which is a long, compound cartilaginous element resulting from the fusion of the centra neural arches (Fig. 2M″–N), as previously described (Nybelin, 1977; Schultze and Arratia, 1986, 1989; Bartsch, 1988; Grande and Bemis, 1998). The bowfin ural neural arch displays similarities with the cartilaginous element present at the distal end of the bichir caudal fin mentioned earlier (Fig. 1L). In our adult bowfin specimens, all neural arches were autogenous (Fig. 1H, Fig. 2N), as in Grande and Bemis’ (1998) specimens. In addition, four pseudo-epurals were developing dorsal to the ural region, posterior to the distal epiphyses of preural neural spine 2 (Fig. 2M″–N). Because they are interposed between neural spines, these ural elements appear to be homologous to pterygiophores and should be designated “epurals” (with quotes) as described by (Schultze and Arratia, 1986); we thus chose to refer to those elements as pseudo-epurals. Both of our adult bowfin had three pseudo-epurals interposed between neural spines and one after the last neural spine (Fig. 1H), in agreement with previous counts (Nybelin, 1977; Schultze and Arratia, 1986; Grande and Bemis, 1998).

In agreement with a previous report of a cartilaginous element uniting the tip of the last haemal spines and all hypurals in bowfin specimens (Schultze and Arratia, 1989), our 99 mm TL specimen displayed an unbroken plate of connective tissue spanning hypaxial elements from the haemal spine 5 to the posterior most hypural (Fig. 2N–N′). Our smallest bowfin (34 mm TL), however, had neither a plate of connective tissue nor distal caudal radials at the distal end of the hypaxial elements (Fig. 2M, M″). In our 99 mm TL bowfin specimen, the fragmentation of the plate of connective tissue, visible at the distal tip of haemal spines 5 and 6, suggests that the plate of connective tissue could have spanned all the hypaxial elements and was fragmenting in an anterior-posterior direction (Fig. 2N′). Notably, the plate of connective tissue was not disrupted between any other adjacent hypural pairs and the fragmentation of the plate of connective tissue didn’t seem to give rise to distal caudal radials (Fig. 2N–N′).

In the 34 mm TL young bowfin hypochordal lobe (the portion of the caudal fin ventral to the notochord), 23 caudal lepidotrichia had already formed, but no lepidotrichia had yet appeared above the notochord (Fig. 2M″). In the 99 mm TL juvenile bowfin, 28 caudal lepidotrichia had formed, including two small epichordal caudal lepidotrichia (Fig. 2N). Both of our adult specimens had 26 caudal lepidotrichia, most of which were branched and segmented, consistent with a prior report of 24 to 32 caudal fin rays (Schultze and Arratia, 1986). Three to four procurrent and one principal ray were present in the adult epichordal lobe (Fig. 1H), also in agreement with previous reports (Nybelin, 1977; Schultze and Arratia, 1986, 1989; Grande and Bemis, 1998).

Spotted gar

The sister group of the bowfin consists of seven species of gar, so gars and bowfin together (Holostei) can inform putative ancestral phenotypes for teleosts. Because development of the spotted gar caudal skeleton has recently been described and compared to other living gar species (Desvignes et al., 2018), here we summarize only the novel observations of gar caudal fin development important to understand caudal fin evolution.

During spotted gar development, the first sign of Alcian uptake in the caudal skeleton appeared by 10–12 mm TL in the first and second hypural rudiments, followed shortly by the parhypural and haemal elements and basiventrals around 14–16 mm TL (Fig. 2I). The upturning of the notochord into the upper lobe, although slight, occurred around 28–32 mm TL, near hypural 1 and was concomitant with the first few hypurals achieving their final cartilaginous shape (Fig. 2J–K). The epurals began to become Alcian positive around 19 mm TL, (Fig. 2K), followed later by mineralization of the dorsal and ventral fulcra around 43 and 125 mm TL respectively (Fig. 2L). The last caudal fin skeletal elements to form were the centra, with the first ural centrum mineralizing around 60 mm TL (Fig. 2L). By 195 mm TL, all structures were as developed and ossified as in our largest adult individual (493 mm TL) (Fig. 1F), with the exception of ural centrum 2 and further posterior centra. These most caudal ural centra continued to ossify slowly after 195 mm TL, and even in the largest individual we studied, the final few ural centra had not mineralized completely and some dorsal arcualia continued to show Alcian uptake (Fig. 1F). The adult caudal fin skeleton was generally organized with six or seven preural centra and up to seven mineralized ural centra, each supporting a haemal spine or a hypural element respectively (Fig. 1F–G). Neural arches and spines formed dorsally on all centra, but were greatly reduced in the ural part of the tail (Fig. 1F). Fully developed spotted gar specimens usually had five epurals positioned in the mesenchyme above the ural centra (Fig. 1F). The notochord in adults exhibited a slight flexion into the upper lobe around ural centrum 1 (Fig. 1F–G).

During development and in adult specimens, hypurals were generally evenly spaced and they decreased in size progressively from anterior to posterior. We observed, however, that the space between hypurals 2 and 3 was generally greater than between other neighboring hypurals, which was more evident in juveniles, and resembled the hypural diastema described in teleosts (Arratia, 2013; Schultze and Arratia, 2013). The size and shape difference between hypurals 2 and 3 was also greater than the difference between any other pair of adjacent hypurals (Fig. 2I–L, Fig. 3A). Although the magnitude of the separation

between hypurals 2 and 3 and the size and shape differences between adjacent hypurals varied among individuals, the position of the separation was consistently at hypurals 2 and 3.

Two plates of connective tissue were separated from each other at the level of hypurals 2 and 3, consistent with the spacing described above, and stained variably with Alcian Blue in many of the smaller specimens (below 85–90 mm TL) (Fig. 8 in (Desvignes et al., 2018)). In order to gain insight into the composition of the plates of connective tissue and test the hypothesis that the plates of connective tissue in gar contain elastin, similarly to zebrafish (Bensimon-Brito et al., 2012a), we performed histological analyses using Orcein staining which specifically stain elastin fibers with a red-rusty color. Histological analysis of the caudal fin with Orcein confirmed that the plates of connective tissue contain elastin fibers (Fig. 3A′, A′1, A′2). Histological sections also confirmed the separation of the plates of connective tissue between hypurals 2 and 3 (Fig. 3A, A′, A′2) and revealed the passage and branching of the caudal vasculature between the two successive hypurals (Fig. 3A′, A′2), as previously observed in spotted gar (e.g. Fig. 6A–B in (Desvignes et al., 2018)). These plates were generally absent in larger specimens (above 85–90 mm TL) and their place was occupied by two types of cartilage distal caudal radials. The anterior and larger plate of connective tissue (pcta) first showed Alcian uptake around 12–14 mm TL and it surrounded and capped the distal epiphyses of the first two hypurals, the parhypural, and haemal spines 2 through 6 or 7 (Fig. 2I–L), in agreement with a described “plate of connective tissue” in the genus *Lepisosteus* (Schultze and Arratia, 1989). In addition to this anterior plate of connective tissue, a previously undescribed smaller secondary, posterior plate (pctp) spanned hypurals 3 to 4 or 5 (Fig. 3K–L and Fig. 8A–B in (Desvignes et al., 2018)). Specimens larger than 85–90 mm TL lacked the plates of connective tissue, but showed in their place two types of distal radials: radials resulting from the separation of the cartilage previously capping the hypaxial elements (post-element distal caudal radials), and smaller radials intercalated between the distal epiphyses of the hypurals and haemal spines encompassed by the plates of connective tissue (intercalated distal caudal radials) (Fig. 8C in (Desvignes et al., 2018)). The consistent presence of intercalated distal caudal radials between hypaxial elements and their systematic absence between hypural 2 and 3 (i.e. at the split between the two plates of connective tissue), drove the conclusion that the intercalated distal caudal radials likely arise from the fragmentation of the two plates of connective tissue (Desvignes et al., 2018).

The earliest-forming caudal lepidotrichia formed at the distal ends of hypurals 1 and 2 (Fig. 2J). Subsequent developing fin rays developed anterior and posterior to the first two lepidotrichia, but the anterior lepidotrichia developed faster than the posterior lepidotrichia, which developed following the formation of the hypural elements with which they associate (Fig. 2J–L). Fully developed gars generally had 12 principle lepidotrichia in their caudal fin that were all branched and segmented, and no procurrent lepidotrichia (Fig. 1F–G), consistent with previous reports (Nybelin, 1977; Schultze and Arratia, 1986; Grande, 2010). No lepidotrichia were present dorsal to the notochord in juvenile or adult gar (Fig. 1F–G), also consistent with previous observations (Nybelin, 1977; Grande, 2010).

Zebrafish

To help understand the evolution of the actinopterygian caudal fin, especially the transition to the teleost homocercal caudal fin, we examined a series of juvenile zebrafish (*Danio rerio*), a teleost that has a homocercal caudal fin and a well-described pattern of skeletal developmental (Fig. 1A) (Bird and Mabee, 2003; Parichy et al., 2009; Bensimon-Brito et al., 2012a; Wiley et al., 2015). In agreement with previous observations, the zebrafish notochord flexed into the dorsal caudal lobe around 8 to 9 dpf (about 4.5 mm TL), and hypural 1 and the parhypural developed early, forming individually around 8 dpf ventral to the flexion point of the notochord (Fig. 2E). Additional hypurals and haemal spines developed in somewhat larger specimens, with all structures extending distally (Fig. 2E–G). Between 9 and 10 dpf (about 5 mm TL), the proximal epiphyses of hypural 1 and the parhypural fused, and the first ural centrum began to mineralize as a compound centrum of preural centrum 1 and ural centra 1 and 2. At about the same age, the opisthural cartilage and the epurals appeared and the central lepidotrichia began to mineralize, forming anterior and posterior to the separation between hypural 2 and 3 (Fig. 2E–G) which is known as the hypural diastema (Arratia, 2013; Schultze and Arratia, 2013). Ural centrum 1 mineralized well before the anterior-to-posterior sequence of mineralizing caudal vertebrae had reached preural centrum 1 (Fig. 2F–G), in agreement with previous observations (Bird and Mabee, 2003; Bensimon-Brito et al., 2012a; b). Around 11 to 12 dpf (about 5.5 mm TL), the uroneurals (un), which are a pair of elongated endochondral bones projecting from the lateral surfaces of the urostyle (ust), began to develop directly into bone (Fig. 2H) and the opisthural cartilage elongated past the posterior margin of the hypurals (Fig. 2H, Fig. 3B), similar to the situation in adults (Fig. 1D). At 13 dpf (about 6 mm TL), the first lepidotrichia started to mineralize dorsal to the notochord and were later represented by four to five procurrent rays (Fig. 1D, Fig. 2H).

Once fully formed, the zebrafish caudal fin skeleton was organized along two individualized preural centra and a compound ural centrum referred as the urostyle; the tail possessed five hypurals, three haemal spines (including the parhypural), two neural spines on the two preural centra, a single epural, and a uroneural (Fig. 1D–E). The presence of two neural arches on the preural centra just anterior to the urostyle (ust in Fig. 1D and Fig. 2H) suggests that this centrum is a compound centrum made of pre-ural centra 2 and 3 (pu2+3), a conclusion that agrees with previous observations (Bensimon-Brito et al., 2010). Two cartilaginous structures (pcta and pctp) that separated from each other at the hypural diastema (i.e. between hypurals 2 and 3) stained with Alcian Blue and capped the distal epiphyses of all hypurals, the paryhpural, and haemal spines 2 and 3 (Fig. 1D, Fig. 3B) and correspond to the plates of connective tissue described in teleosts (Schultze and Arratia, 1988; Arratia and Schultze, 1992; Bensimon-Brito et al., 2012). Similarly to the plates of connective tissue in gar, histological analysis of the caudal fin with an Orcein stain revealed that the plates of connective tissue in zebrafish contain elastin fibers (Fig. 3B′, B′1, B′2). Histological sections also illustrated their separation between hypural 2 and 3 (Fig. 3B, B′, B′2) and revealed the passage and branching of the caudal vasculature between the two successive hypurals (Fig. 3B′, B′2).

Stickleback

To confirm that results from zebrafish are generalizable across teleosts, we studied development of the homocercal caudal fin skeleton of a distantly related teleost, a fresh water strain of three-spined stickleback (*Gasterosteus aculeatus*) (Fig. 1A), which, with a reduced number of structures, possesses a more derived caudal fin endoskeleton than zebrafish. In stickleback, the first developing hypurals had already started to form in contact with the notochord before our earliest observation at 11 dpf (about 6.5 mm TL) (Fig. 2A), in agreement with the report of initial hypural formation around 7.5 dpf (about 5 mm SL) in individuals of the same laboratory strain (Currey et al., 2017). In contrast to the individualized hypurals in zebrafish and spotted gar, hypurals in stickleback developed directly into two hypural plates, with the anterior plate being a compound element of hypural 1 and 2 with the extremities of the parhypural, creating a foramen (Fig. 2A–C), which was also represented in Huxley's drawings of stickleback nearly 160 years ago (Huxley, 1859). The foramen persisted at least up to 30 dpf (about 14–15 mm TL, Fig. 2D), the oldest juveniles we studied before the fully grown individuals in which the foramen is no longer visible (Fig. 1B–C). This foramen likely corresponds to the point of bifurcation of the caudal artery from the haemal canal to the side of the hypurals; a study of the vasculature would answer this question, but this function has been proposed for a similar foramen in tetraodontiformes (Konstantinidis and Johnson, 2012), which are more closely related to stickleback than is zebrafish (Near et al., 2012; Betancur-R et al., 2017). Upward flexion of the notochord started between 14 and 15 dpf (about 7.5–8 mm TL), along with mineralization of the fused centra pu1+u1 (Fig. 2B–C), which followed the mineralization of a fused vertebra pu2+3, evidenced by two neural spines and two haemal elements (Fig. 2A–C), as also seen in Huxley's drawing (Huxley, 1859). Centra mineralized in an anterior-to-posterior progression (Fig. 2A–C). The two hypural plates started to join each other around 14 dpf (about 7.5 mm TL) by a cartilaginous process extending from the posterior plate towards the proximal half of the anterior plate (p-pHP2 in Fig. 2C) and by 30 dpf, the two hypural plates had joined each other proximally (Fig. 2D). Epaxially, the first epural developed in the mesoderm around 11 dpf (about 6.5 mm TL) and the second formed anteriorly to it within a day (Fig. 2C). The epurals eventually fused, similar to the two individualized epurals that are shown fusing and fused later in development in Huxley's seminal work (Huxley, 1859). The epurals fused at their proximal ends during the formation of the second epural (Fig. 2B); the fusion started as early as 14.5 dpf (about 7.5 mm TL) and had occurred by 15.5 dpf (about 8–8.5 mm TL) in half of the stickleback individuals we examined, while mineralization of the compound epural progressed after 30 dpf (Fig. 2D). The first lepidotrichia to mineralize were located at the separation between the two hypural plates, which corresponds to the hypural diastema in stickleback (Arratia, 2013; Schultze and Arratia, 2013), and mineralization progressed in both an anterior and a posterior direction (Fig. 2A–D).

Adult stickleback possessed two hypural plates fused together proximally for about three quarters of their length, reducing the hypural diastema to a notch positioned at the distal regions of hypurals 2 and 3 (Arratia, 2013; Schultze and Arratia, 2013), a urostyle fused with the two hypural plates, and a compound epural formed by the fusion of the two original epurals (Fig. 1B–C). In addition, after 15.5 dpf (about 8–8.5 mm TL), a uroneural fused

anteriorly with the urostyle and saddled posteriorly the dorsal hypural plate (Fig. 1B, Fig. 2D). The general organization of the caudal skeleton was similar to Huxley's stickleback caudal fin representation (Huxley, 1859), ninespine stickleback descriptions (Keivany and Nelson, 1998, 2000) and *Coryphaena* (dolphinfish) drawing (Gosline, 1997). Two plates of connective tissue (pcta and pctp) were present at the distal margin of both hypural plates and each plate of connective tissue articulated with six segmented principal rays (Fig. 1B–C, Fig. 2D). The first preural vertebra pu2+3 had dorsally one large neural spine resulting from the fusion of the two original neural spines, and ventrally two incompletely fused haemal spines (Fig. 1B, Fig. 2D). The two preural vertebrae rostral to pu2+3 both contained one large neural spine and one large haemal spine, but more anterior preural vertebrae had thinner neural and haemal spines (Fig. 1B). Six unbranched and unsegmented procurrent rays articulated both dorsally and ventrally with the posterior-most two neural spines and two haemal spines (Fig. 1B).

Discussion

Analysis of the composition and organization of the caudal fin skeleton in species representing all major actinopterygian lineages revealed that the gar caudal fin displays a hypural diastema complex that is morphologically similar to the one in teleosts, even though the hypural diastema complex had formerly been considered to be a synapomorphy of the Teleostei group. One of at least two hypotheses might explain this finding. According to the "homology by descent" hypothesis, the hypural diastema complex would have originated in a Neopterygian ancestor before the divergence of holostean and teleost lineages followed by the loss of the complex independently in many lineages. Alternatively, the "latent homology hypothesis" suggests that the Neopterygian common ancestor of teleosts and holosteans lacked some or all components of the hypural diastema complex, but possessed underlying developmental and genetic mechanisms that facilitated the emergence of a hypural diastema complex independently in the lineages of both gars and teleosts. This discussion considers evidence from fossils and representative species from all major actinopterygian lineages which appears to support the latent homology hypothesis: the independent and parallel evolution of the hypural diastema complex in gars and teleosts. A major difference between the hypural diastema complex in gars and teleosts, however, is that the gar complex doesn't align with the horizontal body axis in contrast to teleosts. The alignment of the teleost hypural diastema complex with the body axis might have provided functional advantages in maneuverability and/or power. Finally, analysis of the formation of caudal lepidotrichia in gars and teleosts revealed that the earliest caudal lepidotrichia to develop in the embryo directly participates, independent of the hypural diastema complex, in the establishment of external symmetry of the adult caudal fin lobe.

A hypural diastema complex is present in the caudal fin of both gar and teleosts

We show below that a complex of caudal skeletal and mesodermal features previously described only in teleosts is also present in the caudal fin of several gar species. This morphological complex, that we call the "hypural diastema complex", involves three main morphological features: 1) a gap between hypurals 2 and 3, also called the hypural diastema; 2) an anterior and a posterior plate of connective tissue located at the tips of the hypurals

with the break between them at the level of the hypural diastema; and 3) a dorsal-ventral branching of the caudal vasculature at the site of the hypural diastema.

In teleosts, the hypural diastema is defined as a "space positioned between hypurals 2 and 3 (as seen here in zebrafish in Fig. 1D–E, Fig. 2E–H, and Fig. 3B), or a notch positioned at the distal regions of hypurals 2 and 3" (as seen in stickleback in Fig. 1B–C and Fig. 2A–D) (Schultze and Arratia, 2013). This diastema was originally called the "diasteme de Monod" by Schultze and Arratia (Monod, 1968; Schultze and Arratia, 1989), or the "divergence of hypurals 2 and 3" (Metscher and Ahlberg, 2001), and later the "hypural diastema" (Arratia and Schultze, 1992; Schultze and Arratia, 2013). The presence of the hypural diastema in adult fish is a synapomorphy of the basal teleost †*Eurycormus* and more advanced teleosts (Arratia, 2013, 2015). The physical separation between hypurals 2 and 3 consistently corresponds to the position of the gap between the two elastin fiber-containing plates of connective tissue found in many teleosts at the distal ends of haemal spines and hypurals (e.g. pcta and pctp in Fig. 1B–C in stickleback and Fig. 1D–E and Fig. 3B in zebrafish). This gap also marks the location of the dorsoventral branching of the caudal vein and caudal artery between the dorsal and ventral lobes of the teleost caudal fin (Fig. 3B′2)(Schultze and Arratia, 1988; Arratia and Schultze, 1992; Arratia, 2013, 2015; Wiley et al., 2015).

Our preparations unambiguously showed that the gar caudal skeleton displays all three developmental features similar to the hypural diastema in teleosts. In juvenile spotted gar, a physical separation and hypural shape and size difference between hypurals 2 and 3 separates hypaxial elements into two discrete hypaxial ensembles (e.g. Fig. 2I–L, 3A, and (Desvignes et al., 2018)). This space between hypurals 2 and 3 can be considered as a hypural diastema (Schultze and Arratia, 2013). Although the width of the diastema in spotted gar individuals is somewhat variable and tends to be reduced in adults, its relative hypural position is constant. Furthermore, the hypural diastema complex is unambiguously visible in numerous published figures of juvenile gars of various species but has not been pointed out before (e.g., (Nybelin, 1977; Schultze and Arratia, 1986, 1989; Bartsch, 1988; Grande, 2010)). Although visible in those published works, authors did not mention or describe the hypural diastema, likely because, in contrast to adult teleosts, the hypural diastema is difficult to visualize in adult gars due to the weaker flexion of the notochord and the growth and shape of hypurals (Fig. 1F–G and (Desvignes et al., 2018)).

In addition to a hypural diastema, spotted gar possesses two plates of connective tissue on each side of the hypural diastema, between hypurals 2 and 3, from the time they first form in development (Fig. 2I–L, Fig. 3A, and (Desvignes et al., 2018)). Gars had been reported to possess a single plate of connective tissue that spans haemal elements associated with the caudal fin skeleton and the first two hypurals (Schultze and Arratia, 1989; Grande, 2010); this single plate of connective tissue corresponds only to the anterior plate of connective tissue that we observed. The posterior plate of connective tissue, which we described for the first time in a non-teleost actinopterygian fish (Desvignes et al., 2018), is located at the distal end of hypurals 3 to 5 in juvenile gars and appears similar to the posterior plate of connective tissue, or dorsal plate of connective tissue, spanning hypurals 3 to 5 or 6 in teleosts. This posterior plate of connective tissue in juvenile gars was previously thought to be absent in all non-teleost fishes (Schultze and Arratia, 1989). In addition, spotted gar

plates of connective tissue contain elastin fibers (Fig. 3A), similarly to zebrafish (Fig. 3B and (Bensimon-Brito et al., 2012a)), which suggests a similar origin and therefore homology of the plates of connective tissue in gars and teleosts among neopterygians. We also found that in more developed gar individuals, the plates of connective tissue had disappeared and were replaced by distal caudal radials except at the location of the hypural diastema (e.g. Fig. 7 in (Desvignes et al., 2018)). This result is consistent with the hypothesis that distal caudal radials develop from the fragmentation of the two plates of connective tissue, which are separated from each other at the hypural diastema.

Finally, the main caudal vein and artery branch between hypurals 2 and 3 in spotted gar (Fig. 3A′, A′2, and e.g. Fig. 6A–B in (Desvignes et al., 2018)), longnose gar, and shortnose gar (Schultze and Arratia, 1986).

Thus, in summary, we show here for the first time that a hypural diastema complex, an organizational feature of the caudal fin skeleton and mesoderm, is present in the caudal fin of several living species of gar. The hypural diastema complex, in both teleosts and gars, is characterized by 1) a gap between hypurals 2 and 3; 2) two elastin fiber-containing plates of connective tissue that the gap separates, and 3) the dorsal-ventral branch point for the caudal vasculature.

Homology or homoplasy of the hypural diastema complex in gars and teleosts?

The identification of similar morphological complexes associated with the hypural diastema in gars and teleosts raises the question of the evolutionary origin of this anatomical feature. It could be homoplastic and evolved independently in the gar lineage and the teleost lineage after they diverged from a common ancestral state that lacked a hypural diastema complex (Fig. 4A). Alternatively, the complex could be homologous in teleosts and gars, having been present in, and inherited from, their last common ancestor (Fig. 4B). To rule out one of these competing hypotheses, we needed to investigate additional lineages of ray-finned fishes.

The caudal fin of bowfin, paddlefish, and bichir lack a hypural diastema complex

Investigation of bowfin, representing the sister group of gars within the Holostei, and extant basally diverging actinopterygians, including paddlefish and bichir, should help resolve the origin of the organization of the caudal fin around a hypural diastema complex.

Our bowfin individuals displayed no signs of a hypural diastema complex. Each specimen had a single continuous, evenly spaced ensemble of haemal spines and hypural elements (Fig. 1H–I, Fig. 2M–N), consistent with previously published figures (Schultze and Arratia, 1986, 1989; Grande and Bemis, 1998). In addition, our larger juvenile bowfin clearly possessed a unique Alcian-positive plate of connective tissue located at the distal ends of most haemal spines and all hypurals (Fig. 2N), consistent with previous descriptions (Schultze and Arratia, 1989). Unlike teleosts and gars that possess two plates of connective tissue individualized between hypurals 2 and 3, the bowfin plate of connective tissue, however, is unbroken and continuous over all haemal elements, including between hypurals 2 and 3 (Fig. 2N′). Finally, in bowfin, the main caudal veins and arteries do not branch systematically between hypurals 2 and 3, but instead branch at different locations in different individuals (Schultze and Arratia, 1986). The smooth transition of hypural size and position,

the single plate of connective tissue, and the inconsistent location for vascular branching show that the caudal fin skeleton of the living bowfin is not organized around a hypural diastema complex that separates two hypaxial ensembles, but is instead organized in a single united hypaxial ensemble.

Acipenseriformes also provide no evidence for a hypural diastema complex. Our paddlefish samples and other acipenseriformes (Grande and Bemis, 1991; Findeis, 1997; Bemis and Grande, 1999; Metscher and Ahlberg, 2001; Hilton, 2004; Hilton et al., 2011) lacked a clear separation between hypaxial elements (Fig. 1J–K, Fig. 2O–P). Information about the other two characteristics of the hypural diastema complex are missing: to our knowledge, the localization and branching of caudal fin veins and arteries and the existence of one or two plates of connective tissue have never been described in acipenseriformes. Large distal caudal radials, however, are present at the distal epiphyses of the haemal elements and a few hypurals in acipenseriformes (Fig. 1J, Fig. 2P′ and (Bartsch, 1988; Grande and Bemis, 1991)). Given our observation in spotted gars that the fragmentation of the plate of connective tissue gives rise to distal caudal radials (Desvignes et al., 2018), early developmental studies of distal caudal radials in acipenseriformes would be necessary to decipher whether the distal caudal radials observed in paddlefish and sturgeons appear by separation from the distal epiphyses of haemal elements, by independent cartilage cell condensation, or by fragmentation of a plate of connective tissue.

In polypteriformes, the most basally diverging living group of actinopterygians, we observed no signs of a hypural diastema complex (Fig. 1L). Our specimen lacked a distinct separation between any two consecutive hypurals and did not show any plates of connective tissue or distal caudal radials (Fig. 1L), consistent with available literature (Bartsch and Gemballa, 1992). In addition, we are unaware of any description of the vasculature in the caudal fin in polypteriformes.

Together, neither our study nor published studies of living bowfin, paddlefish, and bichir reveal any of the three features of the hypural diastema complex: a gap between morphologically distinct hypurals 2 and 3 (or even between any other adjacent hypurals), a pair of plates of connective tissue, or the branching of caudal veins and arteries between hypurals 2 and 3. We conclude first, that the hypural diastema complex is not shared among all actinopterygians nor the neopterygian subclass, and second, that the complex is not present among all descendants of the most common ancestor of holosteans and teleosts. These observations thus do not permit us to conclude that the hypural diastema complexes in gars and teleosts are homoplastic (Fig. 4A) nor to conclude on the homology in some neopterygians and a secondary loss in bowfin (Fig. 4B), but rule out the possibility that the hypural diastema complex was in place much before the origins of stem Neopterygians.

Some extinct neopterygians may have had a hypural diastema

While living non-teleost actinopterygians provide no evidence for a hypural diastema in a common ancestor of gars and teleosts, the fossil record might provide useful information regarding the origin of the hypural diastema complex (Fig. 4C). Several hurdles, however make fossils difficult tools for the analysis of the hypural diastema complex. First, fossils are unlikely to preserve information on two components of the complex: the vasculature and

either the plates of connective tissue or the cartilaginous distal caudal radials. Second, most neopterygians possess thick ganoid scales covering the entire body that often hide the caudal skeleton. Third, in rare cases where the caudal skeleton is visible, flattening of the specimen often obscures one of the defining characteristic of the first hypural, i.e. the absence of a haemal arch on hypurals, which makes identification of hypurals uncertain. Fourth, much of the basal neopterygian phylogeny remains largely unresolved, and incorrect phylogenies can prevent inference of origins.

Despite these problems, we asked whether signs of a hypural diastema complex, i.e. a gap between two successive hypurals, appear in the holostean lineage (see tree in Fig. 5), which includes other Ginglymodian fishes such as the Semionotiformes and living gars (López-Arbarello, 2012; Gibson, 2016; López-Arbarello and Wencker, 2016), and Halecomorph fishes, for which bowfin is the only living representative (Grande and Bemis, 1998; Brito and Alvarado-Ortega, 2013).

Among Semionotiformes specimens, the caudal endoskeletons is usually not visible because it is covered with scales or doesn't show signs of a hypural diastema (e.g (Cavin and Suteethorn, 2006; López-Arbarello and Sferco, 2011; López-Arbarello, 2012; Schröder et al., 2012; Gibson, 2013; López-Arbarello and Wencker, 2016)). In †*Semionotus elegans*, however, Olsen & McCune (Olsen and McCune, 1991) represented in the caudal skeleton of a specimen a feature that could be a hypural diastema between two hypurals with a pronounced change in hypural shape and size (for elements numbered hypurals 4 and 5 in Figure 12 of (Olsen and McCune, 1991)). Whether the position of the gap and hypural morphology difference is due to difficulties in identifying the first hypural in those specimens or whether they represent a different location than what is found in teleosts and gars is an open question. In either case, this observation suggests that a hypural diastema may have been present in some lineages both in Lepisosteiformes and in Semionotiformes and could therefore be a feature present, more generally, in some Ginglymodian fishes. The rarity of specimens with an accessible caudal skeleton however precludes concluding whether a hypural diastema could be a consistent character of Ginglymodian fishes or not.

The Dapediiform fishes, have been recently suggested to form a sister group to ginglymodians (López-Arbarello, 2012; Thies and Waschkewitz, 2015; Gibson, 2016). In the Dapediiform fish †*Hemicalypterus weiri*, we observed a small gap and a substantial difference in size and orientation of the gap-flanking hypurals called hypurals 5 and 6 (Fig. 7 in (Gibson, 2016)). This gap and change in hypural shape and orientation was not discussed by Gibson, in the article but the author pointed out that "the distinction between hypural and preural haemal spines is difficult to make on laterally compressed fossils" (Gibson, 2016), so one cannot rule out that the gap we observed in †*Hemicalypterus weiri* could be located between hypurals 2 and 3 and could correspond to a hypural diastema.

For the more extended group of holosteans, we reviewed literature on halecomorph fishes, for which bowfin is the only living representative, and which, along with the Ginglymodians, composes the Holostei group (Brito and Alvarado-Ortega, 2013; Xu et al., 2014). As with Ginglymodians, only few halecomorph specimens published in the literature can be studied for their caudal skeleton and most don't display any signs of a hypural

diastema (e.g Fig. 9D in (Ebert et al., 2015), Fig. 6 in (Murray et al., 2013) and (Grande and Bemis, 1998; Murray and Wilson, 2009)). In two articles, however, some specimens show signs that we interpret as a possible hypural diastema. In the ionoscopiform halecomorph †*Quetzalichthys perrilliatae*, a small gap appears between what was labeled hypurals 4 and 5, and these two hypurals show a noticeable difference in hypural curvature (Fig. 6 and Fig. 7B in (Alvarado-Ortega and Espinosa-Arrubarrena, 2008)). Similarly, in published photographs and sketches of the caudal skeleton of †*Cipactlichthys scutatus* (Fig. 9 of (Brito and Alvarado-Ortega, 2013)), which belongs to a distinct group of basal halecomorphs, we observed a previously unmentioned gap between hypurals labeled 4 and 5 and a pronounced change in hypural shape and size between hypurals labeled 4 and 5 that can be interpreted as a hypural diastema. Thus, these two basal halecomorphs of different groups both display a putative hypural diastema, suggesting that a hypural diastema could have been present in some halecomorph lineages but is absent from today's bowfin.

While many other specimens of holosteans do not display any signs of hypural diastema or have inaccessible caudal fin skeleton, together with the presence of a hypural diastema in gars, the presence of what could possibly be a hypural diastema in some other ginglymodians, in a Dapedium, and in halecomorphs shows that a hypural diastema might be a more general feature of at least some holosteans.

The diastema between hypural 2 and 3 is easily identified in the caudal skeleton of almost all living teleosts including the most basally diverging living teleost lineages Elopomorphs and Osteoglossomorphs (Schultze and Arratia, 1988), as well as more basal extinct Teleostei species such as †*Eurycormus speciosus* (Arratia and Schultze, 2007), †*Bavarichthys incognitus* (Arratia and Tischlinger, 2010), and †*Ebertichthys ettlingensis* (Arratia, 2016), and is considered a synapomorphy of the Teleostei (Fig. 5) (Arratia, 2013, 2015). We thus asked whether signs of a hypural diastema could also be found in teleosteomorphs diverging more basal than the Teleostei. Pholidophorid fishes represent the sister group to Teleostei (Fig. 5). In most specimens, we couldn't find any signs of a hypural diastema. In †*Pholidophorus bechei*, however, we observed a clear gap associated with a significant change in hypural sizes associated with the hypurals 2 and 3 in a representation of the caudal skeleton (Fig. 1 in (Patterson, 1968)). In addition, a hypural diastema has been labelled between hypurals 2 and 3 on an interpretative drawing of †*Pholidoctenus serianus* (Fig. 84 in (Arratia, 2013)). The Prohalecites form the sister group to [Pholiphoridians+Teleostei] and are considered the oldest known teleosts (Arratia, 2013, 2015). While Arratia and Tintori clearly mentioned that †*Prohalecites* don't have a hypural diastema between hypurals 2 and 3 (Character 3 in (Arratia and Tintori, 1999)), and most of our observations reach a similar conclusion. In two specimens of †*Prohalecites porroi*, however, a small gap and a change in hypural shape and curvature appear, which we take to be signs of a putative hypural diastema positioned between hypurals 2 and 3 (Fig. 7C in (Tintori, 1990) and Fig. 2 in (Arratia and Tintori, 1999)). Together, signs of a hypural diastema can be found in some Pholidophorids, and possibly in some Prohalecites (Fig. 5), making the hypural diastema a character predating the origin of true Teleostei but perhaps inconsistently present until its fixation and accentuation with the emergence of the Teleostei group.

Because at least some ancestors of the main lineages of holosteans (Ginglymodians, Semionontiforms), and teleosts appear to have a hypural diastema, we checked more basally diverging neopterygian lineages. While the relative divergence order of some neopterygian lineages are as yet unresolved, all phylogenies place holosteans and their sister, the teleosts, as crown groups (e.g. (Xu et al., 2013, 2015; Poyato-Ariza, 2015)). And similarly, as in other groups of fossils, we were generally able to observe signs of a hypural diastema in just a few specimen depictions. A fossil of the stem neopterygian flying fish †*Potanichthys xingyiensis* has features we interpret as a possible hypural diastema: a notch between the posterior most fully visible hypural element and the next element (Fig. 1b in (Xu et al., 2013)). Pycnodonts represent a basal neopterygian lineage (Poyato-Ariza and Wenz, 2002; Poyato-Ariza, 2015) with uncertain identification of the first hypural and confusion of hypurals and haemal spines, which are usually all called “hypochordal elements”. Nonetheless, in an illustration of the pycnodont †*Rhinopycnodus gabriellae*, we interpret signs of a hypural diastema: a gap between hypochordal elements 9 and 10 while all other hypochordal elements are touching each other on their distal ends (Fig. 6–7 in (Taverne and Capasso, 2013a)). If these elements are hypurals 2 and 3, then the first hypural would be the much wider hypochordal element 8. Similarly, in the pycnodont †*Rostropycnodus gayeti*, a clear gap between hypocordal elements 6 and 7 was represented (Fig. 21 in (Taverne and Capasso, 2013b)) and could correspond to a hypural diastema. The three hypurals could therefore correspond to the three last hypochordal elements that the authors described as “moderately broader” (Taverne and Capasso, 2013b). Also, notably, the presence of a ‘diastema’ was used as a derived character in phylogenies of pycnodontiformes (Character 61 in (Poyato-Ariza and Wenz, 2002) and Character 51 in (Poyato-Ariza and Wenz, 2005, p -)), and the authors note “a distinct hypural diastema between hypochordal elements 8 and 9” in the pycnodont †*Coelodua saturnus* (Fig. 27A in (Poyato-Ariza and Wenz, 2002)), while the separation between adjacent hypochordal elements is variable or clearly absent in many other pycnodont lineages (e.g. Fig. 31 in (Poyato-Ariza and Wenz, 2002), Fig. 10A–C in (Ebert et al., 2015)). Many other basal neopterygian lineages, however, can’t be studied due to the covering of the caudal peduncle and caudal fin by scales (e.g. in (Lombardo, 1999; Lin et al., 2011; Sun et al., 2015; Xu et al., 2015)) limiting considerably the inference of presence of a hypural diastema in basal neopterygians.

Taken together, these studies indicate that a hypural diastema may have been present in some basal neopterygians such as Pycnodont fishes, but at variable hypural positions, while in holosteans and basal teleost lineages, when present and/or visible, the hypural diastema appears to be fixed between hypurals 2 and 3.

Parallel evolution and latent homology of the hypural diastema among neopterygians

Taken together, signs of a hypural diastema appear in possibly few basal neopterygians, some holosteans, and in teleosts, but are absent in Acipenseriformes and Polypteriformes, suggesting that a neopterygian ancestor might have had a hypural diastema complex that was lost, perhaps many times, in various lineages including that of today’s bowfin and thus the hypural diastema complex might be homologous between gars and teleosts (Fig. 4B); alternatively, a neopterygian ancestor might have lacked a hypural diastema complex but had instead the underlying genetic and developmental machinery essential for building the

complex and different neopterygian lineages might have independently evolved towards similar morphologies; under this hypothesis the hypural diastema complex would be homoplastic between gars and teleosts (Fig. 4A).

For the gar and teleost hypural diastema complexes to be considered homologous among neopterygians and satisfy the notion of inheritance by ancestry (e.g.(Owen, 1843; Patterson, 1988; Scotland, 2010; Wake et al., 2011; Schultze and Arratia, 2013)), the hypural diastema complex would need to be shared without ambiguity within the monophyletic group of [Holostei+Teleostei] and be present in at least one common ancestor to the same group. Our evidence, while suggesting the existence of a hypural diastema complex in some lineages (i.e. at least gars and teleosts), doesn't confirm the existence of a hypural diastema complex in more basal neopterygians, first, because our observation of the hypural diastema in fossils is interpretative and second, because it is impossible to study both the plates of connective tissue and the caudal vasculature branching in fossils. Therefore, current evidence is insufficient to rule out the hypothesis that the gar and teleost hypural diastema complexes are homologous due to lack of evidence; note also, however, that evidence does not unequivocally show that a hypural diastema complex did exist in a common ancestor to the group [Holostei+Teleostei].

In the incapacity of validating or rejecting the homology status of the gar and teleost hypural diastema complexes, we thus questioned the suitability of the hypothesis of homoplasy of the hypural diastema complexes in gars and teleosts among neopterygians. Among the classes of homoplasy, only reversal (i.e. the re-emergence of an ancestral character that was lost in common ancestors), convergent evolution (i.e. similar forms achieved by different genetic and developmental mechanisms), and parallelism (i.e. similar morphologies having independent origins but similar genetic and developmental bases) can be applied to the hypural diastema complex (atavisms being related to the re-emergence of a structure within a population) (Hall, 2003, 2007; Scotland, 2010; Wake et al., 2011).

Similar to homology among neopterygians, given that no evidence unambiguously shows the existence of a hypural diastema complex in at least one common ancestor to the group [Holostei+Teleostei], we can't conclude that the hypural diastema complex in gars and teleosts among neopterygians is the result of reversal. Available evidence, however, doesn't rule out the hypothesis of reversal and the possibility that the hypural diastema complex might have been once present in a common ancestor, lost in a more recent common ancestor of Teleostei and Holosteans (or independently lost in both lineages after they separated), and subsequently reappeared in Teleostei, in gars and possibly other holostean lineages but not in bowfin.

Because convergence generally involves similar forms achieved by different genetic mechanisms, while parallelism is generally the result of similar morphologies having similar genetic bases (Hall, 2003, 2007; Scotland, 2010; Wake et al., 2011), the anatomical properties of the hypural diastema complex and the close phylogenetic relationship of the studied taxa suggest that the hypural diastema complexes in gars and teleosts are more likely due to parallel evolution of caudal fin skeletal and mesodermal organization among neopterygians rather than the result of convergent evolution if they arose by homoplasy.

In a parallel evolution model, the presence of the hypural diastema complex in gars and teleosts, and putatively among lineages of basal neopterygians (e.g. pycnodontiformes), holosteans, and basal teleosteomoprhs (e.g. Pholidoforiformes), suggests that a caudal organization around a hypural diastema complex could have appeared many times. This recurrent emergence of a hypural diastema complex among a phylogenetic restricted and related group suggests that a common underlying mechanism may exist and could have evolved to produce a similar organization many times. This potency of evolving towards the same morphology has been discussed in the context of uncertain homology and defined in different ways such as the “broad-sense homology” developed by West-Eberhard (West-Eberhard, 2003), “homoiology” by Hennig (Hennig, 1966), “latent homology” by Sir de Beer (de Beer, 1971), or “underlying synapomorphy” by Sæther (Sæther, 1979, 1986; Saether, 1983) which Saether defines as “the inherited capacity to develop parallel similarities” (Sæther, 1986). These views of parallelism and homology focus on evolutionary developmental changes rather than cladistic characters, which traditionally describe homologies to define synapomorphies used to infer relationships between species. The incorporation of an evolutionary developmental perspective approaching the notion of homology at three different levels: morphological, genetic and developmental, decouples phenotype and genotype allowing latency in the appearance of a morphological character among lineages. In that perspective, the homoplasy of the hypural diastema complexes in gars and teleosts, assuming it was not possessed by a common ancestor of the group [Holostei+Teleostei] and therefore potentially arose independently in both lineages, could still be homologous at the genetic level and produced under the control of orthologous patterning genetic pathways, and/or homologous at the developmental level, because it develops with similar anatomical organization, position and developmental dynamics.

In conclusion, the hypural diastema complexes in gars and Teleosts could be the result of homology, reversal homoplasy, or parallel evolution among neopterygians. The absence of evidence showing that a known common ancestor of [Holostei+Teleostei] unambiguously possessed a hypural diastema complex, however, precludes conclusions on the homology and reversal homoplasy status of the hypural diastema complex, without however ruling them out. In contrast the current available evidence appears to fit best the parallel evolution hypothesis. Given the close phylogenetic relationship of the two studied taxa (teleosts and holosteans) and the similarities in development and anatomical features of the hypural diastema complexes in both gars and teleosts, involving the endoskeleton, the mesoderm, and the vasculature, we hypothesize that the hypural diastema complexes in gars and teleosts emerged in parallel from underlying common genetic and development processes that were likely present at the stem of the neopterygian radiation, and independently evolved as a derived morphological character in different lineages such as in pycnodontiformes, gars, and teleosts. Hypural diastema complexes in gars and teleosts can thus be qualified as broad-homologs, homoiologs, or latent homologs.

Participation of the hypural diastema in the establishment of homocercality

To what extent did the emergence of the hypural diastema complex participate in the establishment of the teleost homocercal, dorsoventrally symmetrical caudal fin? This

question gains significance because the spotted gar caudal fin has a hypural diastema complex but is not homocercal.

During actinopterygian evolution, the caudal fin skeleton, and specifically the ural skeleton, shortened: first with the emergence of neopterygians, evident when comparing paddlefish to gar and bowfin (Fig. 1 and 2), then in association with the sharp upturning of the notochord in teleosts (e.g., zebrafish and stickleback Fig. 1 and 2) (Schultze and Arratia, 1986, 1988, 2013; Arratia and Schultze, 1992; Metscher and Ahlberg, 2001; Hilton, 2004; Arratia, 2015). The reduction in ural element number accompanied the association of a few caudal rays with each hypural, which is considered the first caudal skeleton synapomorphy of the teleosteomorph group (Fig. 5) (Arratia, 2013, 2015).

The most striking changes in skeletal elements during the early steps of teleost evolution concern the number of ural centra and associated hypurals. Acipenseriformes and Holostei have a one-to-one relationship between the number of ural centra and the number of hypurals: acipenseriformes can have more than 20 ural centra and hypurals (Bemis and Grande, 1999; Hilton, 2004), we found more than 30 in a young paddlefish (Fig. 1J–K; Fig. 2P–Q), about ten ural centra and ten hypurals in bowfin (Fig. 1H–I; Fig. 2M″–N) (Grande and Bemis, 1998), and about eight in gars (Fig. 1F–G, Fig. 2L and (Nybelin, 1977; Grande, 2010; Desvignes et al., 2018)). In contrast, teleosts have a one-to-several relationship between ural centra and their associated hypurals. In adult teleosts, ural centra are usually reduced to two compound centra and a maximum of six hypurals. Often more derived modern teleost species have fewer than two centra and fewer than six hypurals (Arratia, 2015); for example, zebrafish has just one urostyle and five hypurals and stickleback has one urostyle and two hypural plates (Fig. 1B–E, Fig. 2A–H).

In the reduction of ural elements leading to the teleost homocercal caudal fin, the alignment of the hypural diastema complex in the adult body axis in Teleostei appears to be concomitant with the reduction of ural element number observed in stem-teleosts. While in adult spotted gar, the hypural diastema complex forms an angle of about 10–15 degrees with the body axis (Fig. 1F–G, Fig. 2I–L, Fig. 6B), in contrast, in teleosts, the upturning of the notochord causes the hypural diastema to align secondarily with the anterior-posterior body axis in adults (Fig. 1B–E, Fig. 2A–H, Fig. 6D). In depictions of †*Prohalecites*, the hypural diastema we propose does not seem to align with the body axis; in Pholidophoriformes, however, the hypural diastema seems to align partially with the body axis (Fig. 1 in (Patterson, 1968) and Fig. 75 in (Arratia, 2013)). Direct observations of basal teleosteomorph specimens would be necessary to determine at which point of basal teleost evolution the hypural diastema began to align with the body axis in adults. In teleosts, hypurals connect directly to the notochord; thus, one hypothesis is that the fusion of ural centra into just one or two elements, which reduces the length of the notochord to the point of homocercality, compacted the bases of the hypurals into a reduced area, simultaneously aligning the hypural diastema in the axis of the body. Thus, the positioning of the diastema could simply be the result of a passive hypural re-organization induced by the reduction of the number of ural centra combined with the shortening of the distal part of the notochord.

The hypural diastema complex, however, may have become an enhanced feature in the Teleostei caudal fin compared to the basal teleosteomorphs and gars, because it provided organizational advantages to the mesoderm (e.g. optimal caudal vasculature branching) and/or morphological and mechanistic advantages (enhanced symmetry of the caudal fin for improved swimming capacities). Given that a hypural diastema can be observed in some Pholidoforiforms and gars but isn't aligned with the body axis in adults, while evident and aligned in the Teleostei body axis, then the accentuation of the hypural diastema appears to be concomitant with its positioning in the adult body axis. Therefore, the positioning of the hypural diastema complex in the main body axis may have been the morphological innovation that provides evolutionary advantages leading to the accentuation of the diastema in Teleostei.

The earliest-forming caudal lepidotrichia align with the body axis in both adult gar and teleosts

Actinopterygians with a dorsoventral symmetrical caudal fin achieve symmetry following the flexion of the notochord orienting the lepidotrichia (caudal fin rays) parallel to the anterior-posterior body axis. We thus questioned to which extent the formation of the caudal lepidotrichia is linked to the achievement of dorsoventral symmetry in adults.

What developmental genetic program drives the formation of the earliest forming caudal lepidotrichia at one place or another is not yet understood. In zebrafish (Fig. 2E–F, Fig. 6C), stickleback (Fig. 2A–B), and other teleosts, caudal lepidotrichia develop symmetrically anterior and posterior to hypurals 2 and 3 (Fujita, 1992; Metscher and Ahlberg, 2001; Li et al., 2015), which corresponds to the location of the hypural diastema complex. In spotted gar, however, the earliest-forming lepidotrichia are located around hypural 1 and 2 (Fig. 2J, Fig. 6A and (Desvignes et al., 2018)). Because caudal lepidotrichia originate symmetrically around the hypural diastema in teleosts but not in spotted gar, the anterior-posterior level at which the earliest-forming caudal lepidotrichia develop is not consistently associated with the hypural diastema complex and has thus changed during actinopterygian evolution. This change in position may be linked to the fact that lepidotrichia originate dermally, from the ectoderm, while the hypural diastema complex has a mesodermal origin, and therefore might involve different patterning signals. An understanding of the molecular mechanisms that could coordinate development of the hypural diastema and the earliest lepidotrichia await developmental genetic studies.

Neither our study nor other published investigations have examined sufficient samples of larval and juvenile bowfin (Fig. 2M), paddlefish (Fig. 2O–P), or any other non-teleost actinopterygian, to determine the location of the earliest developing lepidotrichia (Schultze and Arratia, 1986; Grande and Bemis, 1998). Bemis and Grande (1999) provide a sketch of larval paddlefish that shows lepidotrichia originating around the first few hypurals (Bemis and Grande, 1999). For polypteriformes, no information is available concerning the earliest-forming lepidotrichia, but Bartsch and Gembella sketched four caudal fin rays centered around hypural 3 in a juvenile bichir (Fig. 2A in (Bartsch and Gemballa, 1992)). More detailed studies of embryos and larvae from extant non-teleost actinopterygian and basally

diverging teleost taxa would be required to better understand the evolutionary history of the positioning of the earliest-forming caudal lepidotrichia.

In the only two groups for which a detailed developmental description is available (teleosts and gars), we observed that the earliest caudal lepidotrichia correspond to the pair that later becomes directly aligned with the horizontal adult body axis. In zebrafish and stickleback, the earliest lepidotrichia align with the hypural diastema, which itself aligns with the body axis in adults (Fig. 1B–E, Fig. 2A–H, and Fig. 6C–D). In adult spotted gar, we observed that the two earliest lepidotrichia, at hypurals 1 and 2, also align with the axis of the body in adults, although much later in development than in teleosts, while the hypural diastema doesn't align in that orientation and maintain an angle with the earliest-forming lepidotrichia even in adults (Fig. 1F–G, Fig. 2I–L, Fig. 6A–B).

These results demonstrate the shared alignment feature of the earliest-forming lepidotrichia with the adult body axis in both gars and teleosts.

The hypural diastema complex, caudal lepidotrichia, and the evolution of the caudal fin

The caudal fin skeleton of the neopterygian ancestor was organized with each hypural having a one-to-one correspondence with its respective associated ural centrum. Either the hypural diastema complex itself or the developmental genetic potential for the caudal skeleton to evolve and organize independently into a hypural diastema complex in different neopterygian lineages (latent homology) resulted in gars and teleosts having a combination of characters, including the patterning of hypurals 2 and 3 creating a gap between them, the formation of two plates of connective tissue containing elastin fibers, and the caudal vascular branching, that define the hypural diastema complex. In either case, the complex in gar and teleosts likely relies on common underlying genetic mechanisms leading to the presence of similar complexes in different neopterygian lineages. The main difference between the hypural diastema complexes in gars and teleosts is its alignment with the body axis in teleosts, but its alignment dorsal to the body axis in gars. These results show that the hypural diastema complex itself is not a prerequisite for the acquisition of the enhanced teleost dorsoventral caudal fin symmetry; the position of the hypural diastema complex in the axis of the body in adult, however, due perhaps to the shortening of the notochord and the reduction of the number of ural centra, could have provided evolutionary advantages leading to the accentuation of the diastema and its establishment as an important axis of symmetry in the teleost caudal fin. Additionally, in both spotted gar and in teleosts, the earliest-forming caudal lepidotrichia are the ones that align with the adult body axis, suggesting that lepidotrichia alignment is a more ancient conserved feature that is associated with symmetry than is the hypural diastema complex. Altogether, in Teleostei, the hypural diastema complex, by becoming a major anatomical feature aligned with the body axis, likely played an important role in the improved swimming and maneuvering capacities provided by the teleost caudal fin compared to other actinopterygians.

Experimental Procedures

Origin of sampled fish

Spotted gar (*Lepisosteus oculatus*) samples were raised in the University of Oregon fish facility and are the same individuals as those used and described in (Desvignes et al., 2018). Briefly, wild adult spotted gar broodstock was collected by electrofishing from the Atchafalaya River Basin, Louisiana and cultured in a 2 m diameter tank containing artificial spawning substrate under a natural photoperiod. Animals were injected with Ovaprim© (0.5 ml/kg) to induce spawning. Fertilized eggs, embryos, and juveniles were reared in 10-gallon tanks, then in 2m diameter tanks at 24° C, under a 14 h light/10 h dark photoperiod regime. Daily care was performed by the University of Oregon fish facility staff. Paddlefish (*Polyodon spathula*) and bowfin (*Amia calva*) samples were obtained already cleared and stained from the collection of Charles B. Kimmel (University of Oregon). We studied fourteen juvenile paddlefish (from 10–12 mm to 50–65 mm, and 80–85 mm TL), two juvenile bowfin (34 mm and 99 mm TL, stained with Alcian Blue and Alizarin Red), and two adult bowfin (181 mm and 233 mm TL, stained with Alizarin Red only). An adult grey bichir (*Polypterus senegalus*, 161 mm TL) was obtained from a pet store in Eugene, Oregon, USA. Larval, juvenile (6–20 dpf, 4–7 mm TL), and adult (28 mm TL) zebrafish (*Danio rerio*, AB strain) were obtained from the University of Oregon aquatics facility. Three-spined stickleback (*Gasterosteus aculeatus*) of several different ages, juveniles (11–15 dpf, 6.5–8.5 mm TL and 30 dpf, 14–15 mm TL) and an adult (69 mm TL), of a fresh water laboratory strain originating from Boot Lake, Alaska were obtained from Mark Currey in the W. Cresko Laboratory (University of Oregon).

Animals were handled in accordance with good animal practice as approved by the University of Oregon Institutional Animal Care and Use Committee (Animal Welfare Assurance Number A-3009-01, IACUC protocol 12-02RA).

Alcian Blue and Alizarin Red Staining

Briefly, following euthanasia with an overdose of MS-222 (Finquel - Argent Labs), fish were fixed in 4% paraformaldehyde (PFA), washed, and serially transferred into 80% ethanol for storage or immediate staining. Fish were stained first with Alcian Blue for cartilage, enzymatically cleared using 1% trypsin, bleached in 3% hydrogen peroxide, differentially stained with Alizarin Red for bone, and finally cleared with increasing solutions of glycerol (Walker and Kimmel, 2007). Specimens of various species and size were prepared and stained following the same method, but the length of each step was adjusted according to the size of the individual fish.

Observations and Imaging

After staining, fish were observed using a Leica M165 FC stereomicroscope and imaged with a Leica DFC425 C camera for small specimens, or alternatively, for larger specimens, with a Canon EOS60D DSLR mounted with a Canon EF100 mm f/2.8 macro lens.

Histology

Caudal fin regions of 24 mm TL spotted gar larvae (~22 dpf) and 13 mm TL zebrafish (21 dpf) were fixed in 4% PFA, embedded in paraffin wax and sectioned at 7μm. Briefly, sagittal sections were then deparaffinized, rehydrated, stained for 30 min in 1% Orcein dye in 70% ethanol for the presence of elastin fibers (red-rusty color), and counter stained for 40 sec with Gills hematoxylin (blue) before dehydration and mounting. Sections were then observed and imaged on a Leica DFC310 FX camera mounted on a Leica DMLB binocular microscope.

Terminology

Table 1 summarizes the essential terminology of caudal fin skeletal elements based on definitions from (Grande, 2010), from (Schultze and Arratia, 2013), and from ZFIN and Fishbase (Bradford et al., 2011; Froese and Pauly, 2015).

Acknowledgments

Grant Sponsor: This work was funded by the grant NIH 5R01 OD011116 (JHP).

Authors would like to thank Allyse Ferrara and Quenton Fontenot at Nicholls State University for gar fishing and for setting up lab broodstock and laboratory spawns. We thank Ingo Braasch, the University of Oregon Aquatics Facility, Trevor Enright, Andy Kimm, and Tim Mason for gar and zebrafish rearing help; Mark Currey for help in obtaining stickleback and for discussions; Bonnie Ullmann, Jamie Nichols, and Gloria Arratia for insightful comments; Charles B. Kimmel for sharing samples and critical reading of the manuscript; and Ruth Bremiller for advice on histological procedures. We also thank two anonymous reviewers for comments that significantly improved the manuscript. The work was supported by NIH grant 5R01 OD011116 (JHP).

References

Alvarado-Ortega J, Espinosa-Arrubarrena L. A New Genus of Ionoscopiform Fish (Halecomorphi) from the Lower Cretaceous (Albian) Lithographic Limestones of the Tlayúa Quarry, Puebla, Mexico. J Paleontol. 2008; 82:163–175.

Amores A, Force A, Yan Y-L, Joly L, Amemiya C, Fritz A, Ho RK, Langeland J, Prince V, Wang Y-L, Westerfield M, Ekker M, Postlethwait JH. Zebrafish hox Clusters and Vertebrate Genome Evolution. Science. 1998; 282:1711–1714. [PubMed: 9831563]

Arratia G. Identifying patterns of diversity of the actinopterygian fulcra. Acta Zool. 2009; 90:220–235.

Arratia G. Morphology, Taxonomy, and Phylogeny of Triassic Pholidophorid Fishes (Actinopterygii, Teleostei). J Vertebr Paleontol. 2013; 33:1–138.

Arratia G. Complexities of Early Teleostei and the Evolution of Particular Morphological Structures through Time. Copeia. 2015; 103:999–1025.

Arratia G. New remarkable Late Jurassic teleosts from southern Germany: Ascalaboidae n. fam., its content, morphology, and phylogenetic relationships. Foss Rec. 2016; 19:31–59.

Arratia G, Schultze H-P. Reevaluation of the caudal skeleton of certain actinopterygian fishes: III. Salmonidae. Homologization of caudal skeletal structures. J Morphol. 1992; 214:187–249.

Arratia G, Schultze H-P. Eurycormus – Eurypoma, two Jurassic actinopterygian genera with mixed identity. Foss Rec. 2007; 10:17–37.

Arratia G, Schultze HP, Casciotta J. Vertebral column and associated elements in dipnoans and comparison with other fishes: development and homology. J Morphol. 2001; 250:101–172. [PubMed: 11746457]

Arratia G, Tintori A. The caudal skeleton of the Triassic actinopterygian Prohalecites and its phylogenetic position. Mesozoic Fishes 2 - Systematics and Fossil record. 1999:121–142.

Arratia G, Tischlinger H. The first record of Late Jurassic crossognathiform fishes from Europe and their phylogenetic importance for teleostean phylogeny. Foss Rec. 2010; 13:317–341.

Bartsch P. Funktionelle Morphologie und Evolution des Axialskelettes und der Caudalis ursprünglicher Knochenfische. Palaeontogr Abt A. 1988:117–226.

Bartsch P, Gemballa S. On the anatomy and development of the vertebral column and pterygiophores in Polypterus senegalus Cuvier, 1829 (“Pisces”, Polypteriformes). Zool Jahrb Abt Für Anat Ontog Tiere. 1992; 122:497–529.

De Beer G. Homology, an unsolved problem. 1971

Bemis WE, Grande L. Development of the median fins of the North American Paddlefish (Polyodon spatula), and a reevaluation of the lateral fin-fold hypothesis. Mesozoic Fishes 2 - Systematics and Fossil record. 1999:41–68.

Bensimon-Brito A, Cancela ML, Huysseune A, Witten PE. The zebrafish (*Danio rerio*) caudal complex - a model to study vertebral body fusion. J Appl Ichthyol. 2010; 26:235–238.

Bensimon-Brito A, Cancela ML, Huysseune A, Witten PE. Vestiges, rudiments and fusion events: the zebrafish caudal fin endoskeleton in an evo-devo perspective. Evol Dev. 2012a; 14:116–127. [PubMed: 23016979]

Bensimon-Brito A, Cardeira J, Cancela ML, Huysseune A, Witten PE. Distinct patterns of notochord mineralization in zebrafish coincide with the localization of Osteocalcin isoform 1 during early vertebral centra formation. BMC Dev Biol. 2012b; 12:1. [PubMed: 22235774]

Betancur-R R, Broughton RE, Wiley EO, Carpenter K, López JA, Li C, Holcroft NI, Arcila D, Sanciangco M, Cureton JC Ii, Zhang F, Buser T, Campbell MA, Ballesteros JA, Roa-Varon A, Willis S, Borden WC, Rowley T, Reneau PC, Hough DJ, Lu G, Grande T, Arratia G, Ortí G. The tree of life and a new classification of bony fishes. PLoS Curr. 2013:5.

Betancur-R R, Wiley EO, Arratia G, Acero A, Bailly N, Miya M, Lecointre G, Ortí G. Phylogenetic classification of bony fishes. BMC Evol Biol. 2017; 17:162. [PubMed: 28683774]

Bird NC, Mabee PM. Developmental morphology of the axial skeleton of the zebrafish, Danio rerio (Ostariophysi: Cyprinidae). Dev Dyn. 2003; 228:337–357. [PubMed: 14579374]

Bradford Y, Conlin T, Dunn N, Fashena D, Frazer K, Howe DG, Knight J, Mani P, Martin R, Moxon SAT, Paddock H, Pich C, Ramachandran S, Ruef BJ, Ruzicka L, Schaper HB, Schaper K, Shao X, Singer A, Sprague J, Sprunger B, Slyke CV, Westerfield M. ZFIN: enhancements and updates to the zebrafish model organism database. Nucleic Acids Res. 2011; 39:D822–D829. [PubMed: 21036866]

Brito PM, Alvarado-Ortega J. Cipactlichthys scutatus, gen. nov., sp. nov. a New Halecomorph (Neopterygii, Holostei) from the Lower Cretaceous Tlayua Formation of Mexico. PLOS ONE. 2013; 8:e73551. [PubMed: 24023885]

Carpenter CC. Functional Aspects of the Notochordal Appendage of the Young-of-the-Year Gar (Lepisosteus). Proc Okla Acad Sci. 1975; 55:57–64.

Cavin L, Suteethorn V. A New Semionotiform (actinopterygii, Neopterygii) from Upper Jurassic – Lower Cretaceous Deposits of North-East Thailand, with Comments on the Relationships of Semionotiforms. Palaeontology. 2006; 49:339–353.

Cloutier, R., Arratia, G. Early diversity of actinopterygians. In: Arratia, G.Wilson, MVH.Cloutier, R., Schultze, H-P., editors. Recent advances in the origin and early radiation of vertebrates: honoring Hans-Peter Schultze. Muünchen: Verlag Dr. Friedrich Pfeil; 2004. p. 217-270.

Cloutier R, Caron A, Grünbaum T, Le François NR. Effect of Water Velocity on the Timing of Skeletogenesis in the Arctic Charr, Salvelinus alpinus (Salmoniformes: Teleostei): An Empirical Case of Developmental Plasticity. Int J Zool Int J Zool [Internet]. 2011; 2010:2010. Available from: http://www.hindawi.com/journals/ijz/2010/470546/abs/, http://www.hindawi.com/journals/ijz/2010/470546/abs/.

Currey MC, Bassham S, Perry S, Cresko WA. Developmental timing differences underlie armor loss across threespine stickleback populations. Evol Dev. 2017; 19:231–243. [PubMed: 29115024]

Desvignes T, Carey A, Braasch I, Enright T, Postlethwait JH. Skeletal development in the heterocercal caudal fin of spotted gar (Lepisosteus oculatus) and other Lepisosteiformes. Dev Dyn. 2018

Ebert M, Kölbl-Ebert M, Lane JA. Fauna and Predator-Prey Relationships of Ettling, an Actinopterygian Fish-Dominated Konservat-Lagerstätte from the Late Jurassic of Southern Germany. PLOS ONE. 2015; 10:e0116140. [PubMed: 25629970]

Eschmeyer, WN. Catalog of fishes: Genera, Species, References. 2015. Available from: http://researcharchive.calacademy.org/research/ichthyology/catalog/fishcatmain.asp

Faircloth BC, Sorenson L, Santini F, Alfaro ME. A Phylogenomic Perspective on the Radiation of Ray-Finned Fishes Based upon Targeted Sequencing of Ultraconserved Elements (UCEs). PLoS ONE. 2013; 8:e65923. [PubMed: 23824177]

Fiaz AW, Léon-Kloosterziel KM, Gort G, Schulte-Merker S, van Leeuwen JL, Kranenbarg S. Swim-Training Changes the Spatio-Temporal Dynamics of Skeletogenesis in Zebrafish Larvae (Danio rerio). PLOS ONE. 2012; 7:e34072. [PubMed: 22529905]

Findeis, EK. Osteology and phylogenetic interrelationships of sturgeons (Acipenseridae). In: Birstein, VJ.Waldman, JR., Bemis, WE., editors. Sturgeon Biodiversity and Conservation. Developments in Environmental Biology of Fishes. Springer Netherlands; 1997. p. 73-126.Available from: http://link.springer.com/chapter/10.1007/0-306-46854-9_5

Flammang BE, Lauder GV. Caudal fin shape modulation and control during acceleration, braking and backing maneuvers in bluegill sunfish, Lepomis macrochirus. J Exp Biol. 2009; 212:277–286. [PubMed: 19112147]

Froese, R., Pauly, D. FishBase. 2015. Available from: www.fishbase.org

Fujita K. Caudal skeleton ontogeny in the adrianichthyid fish,Oryzias latipes. Jpn J Ichthyol. 1992; 39:107–109.

Gibson SZ. A new hump-backed Ginglymodian fish (Neopterygii, Semionotiformes) from the upper Triassic Chinle formation of Southeastern Utah. J Vertebr Paleontol. 2013; 33:1037–1050.

Gibson SZ. Redescription and Phylogenetic Placement of † Hemicalypterus weiri Schaeffer, 1967 (Actinopterygii, Neopterygii) from the Triassic Chinle Formation, Southwestern United States: New Insights into Morphology, Ecological Niche, and Phylogeny. PLOS ONE. 2016; 11:e0163657. [PubMed: 27657923]

Gosline WA. Functional morphology of the caudal skeleton in teleostean fishes. Ichthyol Res. 1997; 44:137–141.

Grande L. An empirical synthetic pattern study of gars (Lepisosteiformes) and closely related species, based mostly on skeletal anatomy. The resurrection of holostei. American Society of Ichthyologists and Herpetologists Special Publication. 2010:6.

Grande L, Bemis WE. Osteology and Phylogenetic Relationships of Fossil and Recent Paddlefish (Polyodontidae) with comments on the interrelationships of Acipenseriformes. J Vertebr Paleontol. 1991; 11:1–121.

Grande L, Bemis WE. A comprehensive phylogenetic study of amiid fishes (Amiidae) based on comparative skeletal anatomy. An empirical search for interconnected patterns of natural history. J Vertebr Paleontol. 1998; 18:1–690.

Grünbaum, T., Cloutier, R., Dumont, P. Congruence between chondrification and ossification sequences during caudal skeleton development: a Moxostomatini case study. Proc 26th Annu Larval Fish Conf;

Hall BK. Descent with modification: the unity underlying homology and homoplasy as seen through an analysis of development and evolution. Biol Rev. 2003; 78:409–433. [PubMed: 14558591]

Hall BK. Homoplasy and homology: Dichotomy or continuum? J Hum Evol. 2007; 52:473–479. [PubMed: 17434571]

Hennig, W. Phylogenetic Systematics. University of Illinois Press; 1966.

Hilton EJ. The caudal skeleton of Acipenseriformes (Actinopterygii: Chondrostei): recent advances and new observations. Recent advances in the origin and early radiation of vertebrates. 2004:599–617.

Hilton EJ, Grande L, Bemis WE. Skeletal Anatomy of the Shortnose Sturgeon, Acipenser brevirostrum Lesueur, 1818, and the Systematics of Sturgeons (Acipenseriformes, Acipenseridae). Fieldiana Life Earth Sci. 2011:1–168.

Huxley TH. Observations on the Development of some parts of the Skeleton of Fishes. Trans Microsc Soc J. 1859; 7:33–46.

Jaillon O, Aury J-M, Brunet F, Petit J-L, Stange-Thomann N, Mauceli E, Bouneau L, Fischer C, Ozouf-Costaz C, Bernot A, Nicaud S, Jaffe D, Fisher S, Lutfalla G, Dossat C, Segurens B, Dasilva C, Salanoubat M, Levy M, Boudet N, Castellano S, Anthouard V, Jubin C, Castelli V, Katinka M,

Vacherie B, Biémont C, Skalli Z, Cattolico L, Poulain J, de Berardinis V, Cruaud C, Duprat S, Brottier P, Coutanceau J-P, Gouzy J, Parra G, Lardier G, Chapple C, McKernan KJ, McEwan P, Bosak S, Kellis M, Volff J-N, Guigó R, Zody MC, Mesirov J, Lindblad-Toh K, Birren B, Nusbaum C, Kahn D, Robinson-Rechavi M, Laudet V, Schachter V, Quétier F, Saurin W, Scarpelli C, Wincker P, Lander ES, Weissenbach J, Crollius HR. Genome duplication in the teleost fish Tetraodon nigroviridis reveals the early vertebrate proto-karyotype. Nature. 2004; 431:946–957. [PubMed: 15496914]

Keivany Y, Nelson JS. Comparative Osteology of the Greek Ninespine Stickleback, Pungitius hellenicus (Teleostei, Gasterosteidae). J Ichtyology. 1998; 38:430–440.

Keivany Y, Nelson JS. Taxonomic review of the genus Pungitius ninespine sticklebacks (Gasterosteidae). Cybium. 2000; 24:107–122.

Komagata K, Suzuki A, Kuwabara R. Sexual dimorphism in the polypterid fishes,Polypterus senegalus andCalamoichthys calabaricus. Jpn J Ichthyol. 1993; 39:387–390.

Konstantinidis P, Johnson GD. A comparative ontogenetic study of the tetraodontiform caudal complex: Caudal complex of tetraodontiforms. Acta Zool. 2012; 93:98–114.

Lauder GV. Function of the Caudal Fin During Locomotion in Fishes: Kinematics, Flow Visualization, and Evolutionary Patterns. Am Zool. 2000; 40:101–122.

Li I-J, Chang C-J, Liu S-C, Abe G, Ota KG. Postembryonic staging of wild-type goldfish, with brief reference to skeletal systems. Dev Dyn. 2015; 244:1485–1518. [PubMed: 26316229]

Lin H, Sun Z, Tintori A, Lombardo C, Jiang D, Hao W. A new species of Habroichthys Brough, 1939 (Actinopterygii; Peltopleuriformes) from the Pelsonian (Anisian, Middle Triassic) of Yunnan Province, South China. Neues Jahrb Fr Geol Palontologie - Abh. 2011; 262:79–89.

Lombardo C. Sexual dimorphism in a new species of the actinopterygian Peltopleurus from the Triassic of northern Italy. Palaeontology. 1999; 42:741–760.

López-Arbarello A. Phylogenetic Interrelationships of Ginglymodian Fishes (Actinopterygii: Neopterygii). PLOS ONE. 2012; 7:e39370. [PubMed: 22808031]

López-Arbarello A, Sferco E. New semionotiform (Actinopterygii: Neopterygii) from the Late Jurassic of southern Germany. J Syst Palaeontol. 2011; 9:197–215.

López-Arbarello A, Wencker LCM. New callipurbeckiid genus (Ginglymodi: Semionotiformes) from the Tithonian (Late Jurassic) of Canjuers, France. PalZ. 2016; 90:543–560.

Metscher, BD., Ahlberg, PE. Systematics Association. Origin of the teleost tail: phylogenetic frameworks for developmental studies. In: Ahlberg, PE., editor. Major events in early vertebrate evolution: palaeontology, phylogeny, genetics, and development. The Systematics Association special volume series. London; New York: Taylor & Francis; 2001. p. 343-349.

Monod T. Le Complexe urophore des poissons téléostéens. IFAN. 1968

Moriyama Y, Takeda H. Evolution and development of the homocercal caudal fin in teleosts. Dev Growth Differ. 2013 n/a–n/a.

Murray AM, Wilson MVH. A New Late Cretaceous Macrosemiid Fish (neopterygii, Halecostomi) from Morocco, with Temporal and Geographical Range Extensions for the Family. Palaeontology. 2009; 52:429–440.

Murray, AM., Wilson, MVH., Gibb, S., Chatterton, BDE. Mesozoic fishes 5 - Global diversity and evolution. München; 2013. Additions to the Late Cretaceous (Cenomanian/Turonian) actinopterygian fauna from the Agoult locality, Akrabou Formation, Morocco, and comments on the palaeoenvironment; p. 525-548.Available from: https://www.researchgate.net/publication/258486528_Additions_to_the_Late_Cretaceous_CenomanianTuronian_actinopterygian_fauna_from_the_Agoult_locality_Akrabou_Formation_Morocco_and_comments_on_the_palaeoenvironment

Near TJ, Dornburg A, Tokita M, Suzuki D, Brandley MC, Friedman M. Boom and Bust: Ancient and Recent Diversification in Bichirs (polypteridae: Actinopterygii), a Relictual Lineage of Ray-Finned Fishes. Evolution. 2014; 68:1014–1026. [PubMed: 24274466]

Near TJ, Eytan RI, Dornburg A, Kuhn KL, Moore JA, Davis MP, Wainwright PC, Friedman M, Smith WL. Resolution of ray-finned fish phylogeny and timing of diversification. Proc Natl Acad Sci U S A. 2012; 109:13698–13703. [PubMed: 22869754]

Nelson, JS. Fishes of the world. 4. Hoboken, N.J: John Wiley; 2006.

Nybelin O. The Polyural Skeleton of Lepisosteus and Certain Other Actinopterygians. Zool Scr. 1977; 6:233–244.

Olsen PE, McCune AR. Morphology of the Semionotus elegans species group from the Early Jurassic part of the Newark Supergroup of eastern North America with comments on the Family Semionotidae (Neopterygii). J Vertebr Paleontol. 1991; 11:269–292.

Owen, R. Lectures on the comparative anatomy and physiology of the invertebrate animals, delivered at the Royal college of surgeons, in 1843. London: Longman, Brown, Green, and Longmans; 1843.

Parichy DM, Elizondo MR, Mills MG, Gordon TN, Engeszer RE. Normal table of postembryonic zebrafish development: Staging by externally visible anatomy of the living fish. Dev Dyn. 2009; 238:2975–3015. [PubMed: 19891001]

Patterson C. Homology in classical and molecular biology. Mol Biol Evol. 1988; 5:603–625. [PubMed: 3065587]

Patterson, colin. The caudal skeleton in Lower Liassic pholidophorid fishes. Bull Br Mus Nat Hist Geol. 1968; 16:201–239.

Postlethwait JH, Yan YL, Gates MA, Horne S, Amores A, Brownlie A, Donovan A, Egan ES, Force A, Gong Z, Goutel C, Fritz A, Kelsh R, Knapik E, Liao E, Paw B, Ransom D, Singer A, Thomson M, Abduljabbar TS, Yelick P, Beier D, Joly JS, Larhammar D, Rosa F, Westerfield M, Zon LI, Johnson SL, Talbot WS. Vertebrate genome evolution and the zebrafish gene map. Nat Genet. 1998; 18:345–349. [PubMed: 9537416]

Poyato-Ariza, FJ. Studies on Pycnodont Fishes (I): Evaluation of their Phylogenetic Position among Actinopterygians; Riv Ital Paleontol E Stratigr Res Paleontol Stratigr [Internet]. 2015. p. 121Available from: http://riviste.unimi.it/index.php/RIPS/article/view/6521

Poyato-Ariza FJ, Wenz S. A new insight into pycnodontiform fishes. Geodiversitas. 2002; 24:139–248.

Poyato-Ariza FJ, Wenz S. Akromystax tilmachiton gen. et sp. nov., a new pycnodontid fish from the Lebanese Late Cretaceous of Haqel and En Nammoura. J Vertebr Paleontol. 2005; 25:27–45.

Sæther OA. Underlying Synapomorphies and Anagenetic Analysis. Zool Scr. 1979; 8:305–312.

Saether OA. The Canalized Evolutionary Potential: Inconsistencies in Phylogenetic Reasoning. Syst Zool. 1983; 32:343–359.

Sæther OA. The Myth of Objectivity—Post-Hennigian Deviations. Cladistics. 1986; 2:1–13.

Sallan LC. Major issues in the origins of ray-finned fish (Actinopterygii) biodiversity. Biol Rev. 2014; 89:950–971. [PubMed: 24612207]

Schröder KM, López-Arbarello A, Ebert M. Macrosemimimus, gen. nov. (Actinopterygii, Semionotiformes), from the Late Jurassic of Germany, England, and France. J Vertebr Paleontol. 2012; 32:512–529.

Schultze H-P, Arratia G. Reevaluation of the caudal skeleton of actinopterygian fishes: I. Lepisosteus and Amia. J Morphol. 1986; 190:215–241.

Schultze H-P, Arratia G. Reevaluation of the caudal skeleton of some actinopterygian fishes: II. Hiodon, Elops, and Albula. J Morphol. 1988; 195:257–303.

Schultze H-P, Arratia G. The composition of the caudal skeleton of teleosts (Actinopterygil: Osteichthyes). Zool J Linn Soc. 1989; 97:189–231.

Schultze, H-P., Arratia, G. The caudal skeleton of basal teleosts, its conventions, and some of its major evolutionary novelties in a temporal dimension. In: Wilson, MVH.Arratia, G., Schultze, H-P., editors. Mesozoic fishes 5 - Global diversity and evolution. München: F. Pfeil; 2013. p. 187-246.

Scotland RW. Deep homology: A view from systematics. BioEssays. 2010; 32:438–449. [PubMed: 20394064]

Sun Z-Y, Lombardo C, Tintori A, Jiang D-Y. A New Species of Altisolepis (Peltopleuriformes, Actinopterygii) from the Middle Triassic of Southern China. J Vertebr Paleontol. 2015; 35:e909819.

Taverne, L., Capasso, L. Osteology and relationships of Rhinopycnodus gabriellae gen. et sp. nov. (Pycnodontiformes) from the marine Late Cretaceous of Lebanon. Eur J Taxon [Internet]. 2013a. Available from: http://www.europeanjournaloftaxonomy.eu/index.php/ejt/article/view/190

Taverne, L., Capasso, L. Gladiopycnodontidae, a new family of pycnodontiform fishes from the Late Cretaceous of Lebanon, with the description of three genera. Eur J Taxon [Internet]. 2013b. Available from: http://www.europeanjournaloftaxonomy.eu/index.php/ejt/article/view/178

Taylor JS, Braasch I, Frickey T, Meyer A, de Peer YV. Genome Duplication, a Trait Shared by 22,000 Species of Ray-Finned Fish. Genome Res. 2003; 13:382–390. [PubMed: 12618368]

Thies, D., Waschkewitz, J. Redescription of Dapedium pholidotum (Agassiz, 1832) (Actinopterygii, Neopterygii) from the Lower Jurassic Posidonia Shale, with comments on the phylogenetic position of Dapedium Leach, 1822. J Syst Palaeontol [Internet]. 2015. Available from: http://www.tandfonline.com/doi/abs/10.1080/14772019.2015.1043361

Tintori A. The actinopterygian fish Prohalecites from the Triassic of northern Italy. Palaeontology. 1990; 33:155–174.

Wake DB, Wake MH, Specht CD. Homoplasy: From Detecting Pattern to Determining Process and Mechanism of Evolution. Science. 2011; 331:1032–1035. [PubMed: 21350170]

Walker M, Kimmel C. A two-color acid-free cartilage and bone stain for zebrafish larvae. Biotech Histochem. 2007; 82:23–28. [PubMed: 17510811]

Wanninger A. Morphology is dead – long live morphology! Integrating MorphoEvoDevo into molecular EvoDevo and phylogenomics. Evol Dev Biol. 2015; 3:54.

West-Eberhard, MJ. Developmental Plasticity and Evolution. Oxford University Press; 2003.

Wiley EO, Fuiten AM, Doosey MH, Lohman BK, Merkes C, Azuma M. The Caudal Skeleton of the Zebrafish, Danio rerio, from a Phylogenetic Perspective: A Polyural Interpretation of Homologous Structures. Copeia. 2015; 103:740–750. [PubMed: 28250540]

Xu G-H, Gao K-Q, Coates MI. Taxonomic revision of Plesiofuro mingshuica from the Lower Triassic of northern Gansu, China, and the relationships of early neopterygian clades. J Vertebr Paleontol. 2015; 35:e1001515.

Xu G-H, Zhao L-J, Coates MI. The oldest ionoscopiform from China sheds new light on the early evolution of halecomorph fishes. Biol Lett. 2014; 10:20140204. [PubMed: 24872460]

Xu G-H, Zhao L-J, Gao K-Q, Wu F-X. A new stem-neopterygian fish from the Middle Triassic of China shows the earliest over-water gliding strategy of the vertebrates. Proc R Soc Lond B Biol Sci. 2013; 280:20122261.

Key findings

1. The hypural diastema complex is an anatomical landmark associated with 1) a gap between hypurals 2 and 3; 2) the separation of two plates of connective tissue present at the distal epiphyses of hypaxial elements; and 3) the corridor and branching point of the caudal vasculature.
2. Gar and teleost caudal fins are both organized with a hypural diastema complex.
3. Gar and teleost hypural diastema complexes are likely latent homologs among neopterygians rather than as previously thought a teleost synapomorphy.
4. The earliest-forming caudal fin rays participate in the establishment of dorsoventral caudal fin symmetry in adult gar and teleosts.
5. These findings revise our understanding of the evolution of the actinopterygian caudal fin, an organ that provides teleosts with advanced maneuverability and powerful swimming compared to non-teleost actinopterygians.

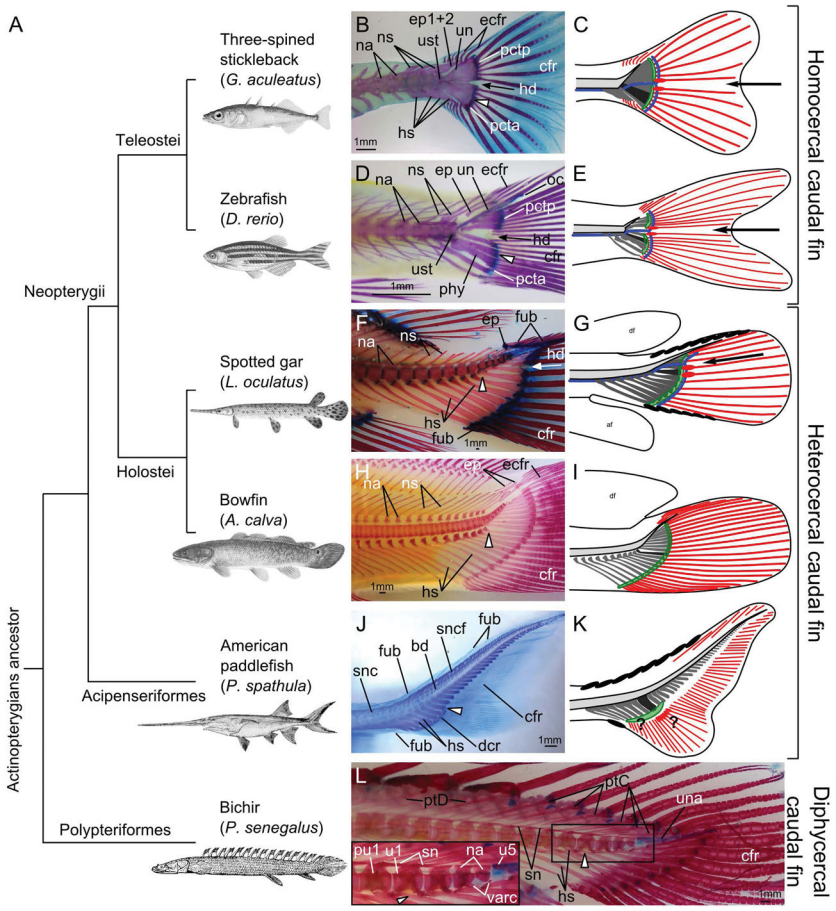

Figure 1.

Evolution of the caudal fin skeleton in actinopterygians. (A) Phylogenetic relationships of actinopterygians investigated here (after (Near et al., 2012, 2014; Betancur-R et al., 2013, 2017)). (B, D, F, J, L) Alcian Blue and Alizarin Red cleared and stained skeletons. (H) Alizarin Red cleared and stained skeleton. (B, C) Adult three-spined stickleback (*Gasterosteus aculeatus*), 69 mm TL. (D–E) Adult zebrafish (*Danio rerio*), 28 mm TL. (F–G) Adult spotted gar (*Lepisosteus oculatus*), 493 mm TL. (H–I) Adult bowfin (*Amia calva*) 233 mm TL. (J–K) Young American paddlefish (*Polyodon spathula*), 84 mm TL. (L) Adult bichir (*Polypterus senegalus*), 161 mm TL. For each species, the white elongated triangle indicates hypural 1 as a reference. In B–G, the arrow points to the hypural diastema. Scale bars represent 1 mm. Abbreviations: bd, basidorsal arcualia; cfr, caudal fin rays; dcr, distal caudal radials; ecfr, epichordal caudal fin rays; ep, epurals; ep1+2, compound epural made by the fusion of epurals 1 and 2; fub, basal fulcra; hd, hypural diastema; hs, haemal spines; oc, opisthural cartilage; na, neural arches; ns, neural spine; phy, parhypural; pcta, anterior plate of connective tissue; pctp, posterior plate of connective tissue; ptC, pterygiophores of the caudal fin; ptD, pterygiophores of the dorsal fin; pu1, preural centrum 1; sn, supraneurals; snc, supraneurals of the caudal skeleton; sncf, supraneurals of the caudal fin skeleton; un, uroneural; una, ural neural arch; ust, urostyle; u1, ural centrum 1; u5, ural centrum 5; varc, ventral arcualia. In the schematic representations of caudal fin organization (C, E, G, I, K), the notochord is represented in light grey, the haemal elements in dark grey,

and the first hypural in black. Plate(s) of connective tissue are represented in green. A black arrow points at the hypural diastema in teleosts (C, E) and gar (G). Caudal vasculature is represented in blue in teleosts (C, E) and gar (G) based on literature and previously published information (Schultze and Arratia, 1986, 1988; Arratia and Schultze, 1992; Arratia, 2013, 2015; Wiley et al., 2015; Desvignes et al., 2018) as well as histological observations in zebrafish and gar (cf. Fig. 3); the vasculature is not shown for bowfin (I) and paddlefish (K) because it is unknown or inconsistently positioned. Caudal lepidotrichia are represented in red, with the earliest-forming lepidotrichia marked with an oval at their base. Fulcra are represented with plain black ovals on the dorsal and/or ventral leading edge of the fin in gar (G) and paddlefish (K). Question marks in paddlefish (K) denote uncertainty concerning the plate of connective tissue and the earliest-forming caudal lepidotrichia. Abbreviations: af, anal fin; df, dorsal fin.

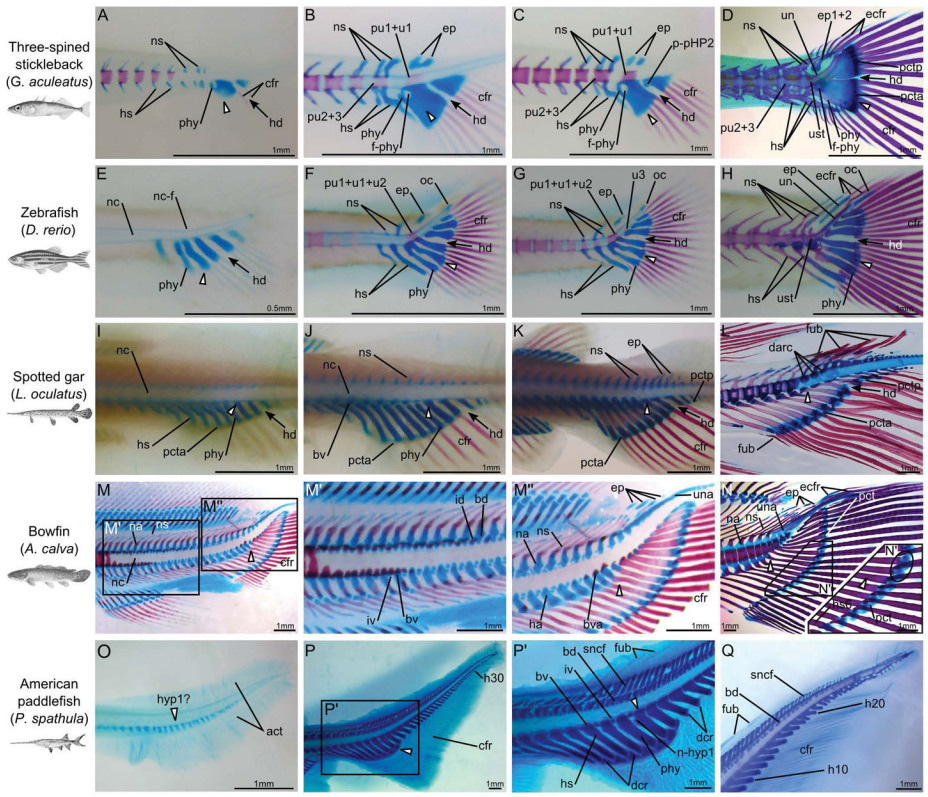

Figure 2.

Developmental details of the caudal fin skeleton in stickleback, zebrafish, spotted gar, bowfin, and American paddlefish. (A–D) Three-spined stickleback (*Gasterosteus aculeatus*), 6.5 mm TL (A), 7 mm TL (B), 7.5 mm TL (C) and 15 mm TL (D). (E–H) Zebrafish (*Danio rerio*) 4.5 mm TL (E), 5 mm TL (F), 5.5 mm TL (G), and 6 mm TL (H). (I–L) Spotted gar (*Lepisosteus oculatus*), 17 mm TL (I), 19 mm TL (J), 26 mm TL (K), and 85 mm TL (L). (M–N) Bowfin (*Amia calva*), 34 mm TL (M–M″) and 99 mm TL (N). (O–Q) American paddlefish (*Polyodon spathula*), 12 mm TL (O), 65 mm TL (P–P′) and 85 mm TL (Q). (L) is a detail of the posterior part of the notochord of Fig. 1J. For each species, the white elongated triangle indicates hypural 1 as a reference. In A–L the black arrow points at the hypural diastema. In the insert in (N), the oval circles the distal ends of hypurals 2 and 3 showing an unbroken plate of connective tissue. Abbreviations: act, actinotrichia; bd, basidorsal arcualia; bv, basiventral arcualia; bva, basiventral autocentra; cfr, caudal fin rays; darc, dorsal arcualia; dcr, distal caudal radials; ecfr, epichordal caudal fin rays; ep, epurals; ep1+2, compound epural made by the fusion of epurals 1 and 2; f-phy, foramen created by the parhypural; fub, basal fulcra; ha, haemal arches; hd, hypural diastema; hs, haemal spines; hyp1?, putative hypural 1; h10, hypural 10; h20, hypural 20; h30, hypural 30; id, interdorsal arcualia; iv, interventral arcualia; oc, opisthural cartilage; n-hyp1, notch at the base of hypural 1; na, neural arches; nc, notochord; nc-f, notochord point of flexion; ns, neural spine; phy, parhypural; pct, plate of connective tissue; pcta, anterior plate of connective tissue; pctp, posterior plate of connective tissue; p-pHP2, anterior process of the posterior hypural plate; pu1+u1, compound centrum made by the fusion of preural centrum 1 and ural centrum 1; pu2+3, compound centrum made by the fusion of preural centra 2 and 3;

pu1+u1+u2, compound centrum made by the fusion of preural centrum 1 and ural centra 1 and 2; sncf, supraneurals of the caudal fin skeleton; un, uroneural; una, ural neural arch; ust, urostyle; u3, ural centrum 3.

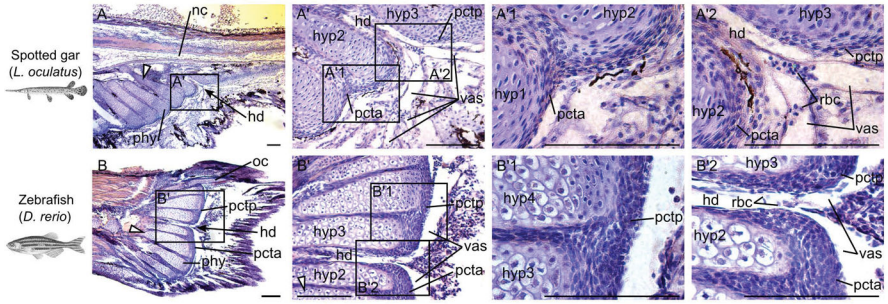

Figure 3.

Orcein stains for elastin in plates of connective tissue in spotted gar and zebrafish. Sagittal sections of caudal fin regions of (A) a 24 mm TL spotted gar larva (~22 dpf) and (B) a 13 mm TL zebrafish (21 dpf) stained with Orcein (red-rusty color) and counter stained with Gills hematoxylin (blue-purple). Scale bar is 100 μm. White elongated triangles indicate hypural 1 and black arrows point at the hypural diastema. Abbreviations: hd, hypural diastema; hyp, hypural; nc, notochord; oc, opisthural cartilage; pcta, anterior plate of connective tissue; pctp, posterior plate of connective tissue; phy, parhypural; rbc, red blood cells; vas, vasculature.

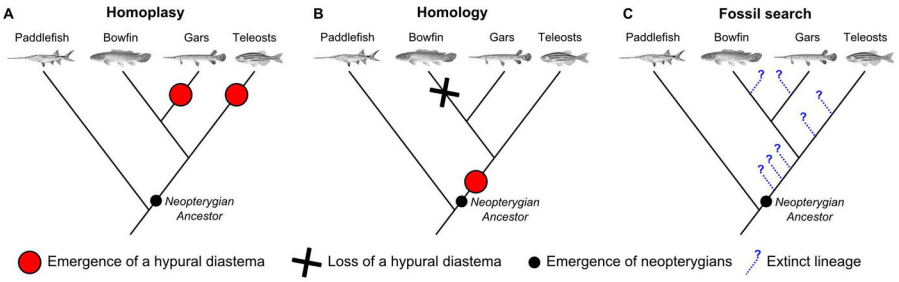

Figure 4.

Evolutionary scenarios for the origin of the hypural diastema complex. (A) Homoplasy scenario, (B) Homology scenario, (C) Search for extinct livening species that can inform the ancestral state for the hypural diastema. Plain red circles denote the emergence of a hypural diastema, the X represents the loss of a hypural diastema, the small plain black circle represents the emergence of neopterygians, and blue dotted lines finished by a question mark relate to extinct lineages represented only by fossils. Tree topology based on (Near et al., 2012; Betancur-R et al., 2013).

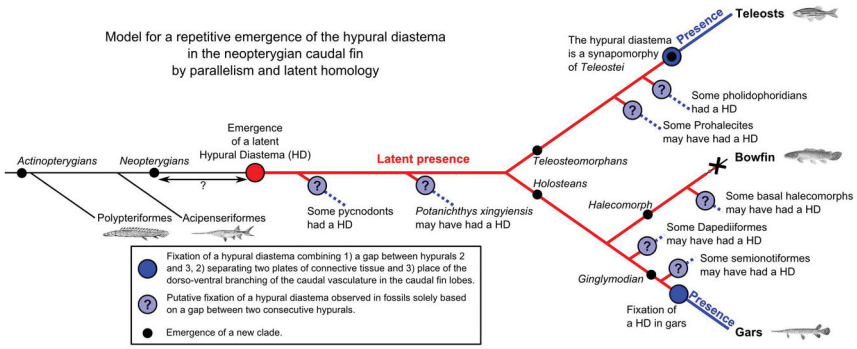

Figure 5.

Parallel evolution by latent homology of the hypural diastema (HD) in neopterygians. The plain red circle denotes the latent emergence of a hypural diastema in basal neopterygians. The plain dark blue circles denote the fixation of the hypural diastema complex in teleost and gar lineages. Plain light blue circles with a question mark inside represent the putative fixation of the hypural diastema complex in fossil lineages suggested by signs of a hypural diastema visible in the caudal fin skeleton. The X represents the absence of the hypural diastema in bowfin; the small plain black circles represent the emergence of new clades.

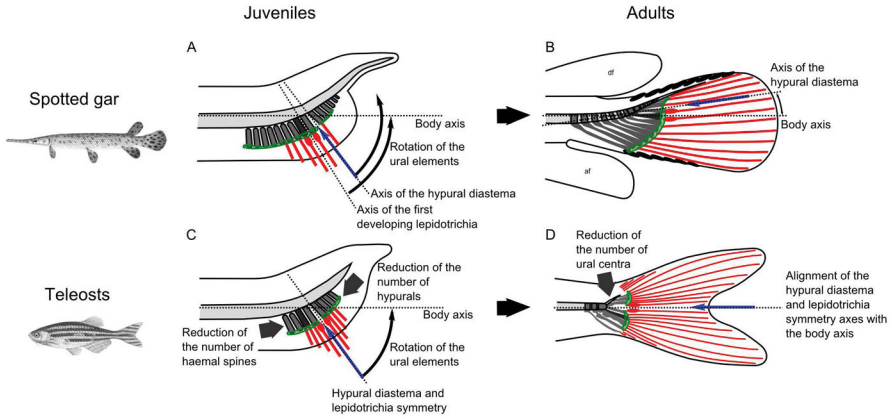

Figure 6.

Position of the hypural diastema and the earliest developing caudal lepidotrichia in juveniles (A–C) and adults (B–D) of spotted gar (A–B) and teleosts (C–D). Zebrafish (*Danio rerio*) is here used as a representative teleost. The notochord is represented in light grey, the haemal elements are in dark grey with the first hypural in black. Plates of connective tissue are represented by a green shape. A blue arrow points at the hypural diastema in teleosts and gar. Caudal lepidotrichia are represented in red with the earliest developing lepidotrichia marked with an oval at their base. Dotted lines represent the main axis of the species' body. Fulcra are represented with plain black ovals on the dorsal and ventral leading edge of the fin in gar (B). Abbreviations: af, anal fin; df, dorsal fin.

Table 1

Caudal fin skeleton terminology.

Term	Symbol	Definition
Actinotrichia	act	Slender rods of collagen (i.e. elastoidin) that are the main support of the fin-folds in young stages, and around which lepidotrichia later develop, while remaining at the tip lepidotrichia in adults.
Basidorsal arcualia	darc	Small paired cartilaginous dorsal vertebral elements forming the bases of the neural arch; the neural arch, which ossifies, is an extension of this element; also called basidorsal cartilage or basidorsals.
Basiventral arcualia	bv	Small paired cartilaginous ventral vertebral elements forming the bases of the haemal arch; the haemal arch, which ossifies, is an extension of this element; also called basiventral cartilage or basiventrals.
Caudal fin skeleton		Posterior-most portion of the axial skeleton. The anterior-most caudal fin skeleton centra support the anterior-most haemal element that supports a caudal fin ray (Fig. 1B). The caudal fin skeleton is subdivided into two regions: the preural and ural regions defined by the nature of the centra (Fig. 1B).
Caudal skeleton		Portion of the axial skeleton located posterior to the abdominal skeleton and anterior to the caudal fin skeleton.
Centrum	c	Refers to the central body of each vertebra; represented by mineralized, calcified, or ossified portions of the vertebra that surround the notochord.
Distal caudal radials	dcr (pdcr and idcr)	Small caudal skeletal elements located distal to the proximal radials (haemal elements and hypurals). Several types of distal caudal radials can be present, including here in gar the “post-element distal caudal radials” (pdcr) and the “intercalated distal caudal radials” (idcr).
Diural caudal skeleton		A type of caudal skeleton commonly found in adult teleosts and characterized by the presence of exactly two ural centra.
Embryonic fin fold	ff	Median skin fold surrounding the body within which the dorsal, anal and caudal fins develop.
Epaxial elements		Skeletal elements positioned dorsal to the notochord/vertebral column (e.g. neural spines and epurals).
Epichordal and hypochordal lobes	el and hl	Caudal fin lobes located dorsal (epi-) or ventral (hypo-) to the notochord (nc).
Epurals	ep	Autonomous neural spines of a preural or ural vertebra that may support fin rays.
Fulcra	pfub, fub, and fufr	Modified scales located at the margins of fins. In extant species, they are present only in acipenseriformes and gars. Fulcra can be divided into two main types: basal fulcra, which can be paired (pfub) or individual (fub) and are present on both the dorsal and ventral bases of the caudal fin, and fringing fulcra (fufr), which border the marginal rays of the caudal fin. In the present study, we use Arratia’s definition of fulcra (Arratia, 2009), and not that of Grande (Grande, 2010), who interpreted paired basal fulcra as rudimentary fin rays and used the name basal fulcra solely for unpaired elements.
Haemal arches	ha	Ventral arches of a caudal vertebrae enclosing, in the haemal canal, the main arteries and veins of the caudal region.
Haemal elements		Refers to the compound elements formed by a haemal spine and a haemal arch.
Haemal spines	hs	Ventral extension of the haemal arch forming the haemal element with the haemal arch.
Hypaxial elements		Skeletal elements positioned ventral to the notochord/vertebral column (e.g. haemal elements and hypurals).
Hypural	hyp	Modified haemal spine that is associated with a ural centrum and has lost its haemal arch and haemal canal; may be articulated or fused with its respective ural centrum.
Hypural diastema		The physical gap located between hypurals 2 and 3. In some teleost species, only a notch positioned at the distal regions of compound element formed by the hypurals remains.
Hypural diastema complex		An anatomical landmark associated with 1) a physical separation between hypurals 2 and 3 (the Hypural diastema); 2) the point of separation between the two plates of connective tissue present at the distal epiphyses of hypaxial elements; and 3) the passage way and branching point of the caudal arteries and veins.
Interdorsal arcualia	Id	Paired cartilaginous dorsal vertebral elements that form between the basidorsal arcualia.

Term	Symbol	Definition
Interventral arcualia	iv	Paired cartilaginous ventral vertebral elements that form between the basiventral arcualia.
Lepidotrichia or caudal fin rays	cfr	Bony segmented fin rays found in bony fishes. They develop around actinotrichia as part of the dermal exoskeleton.
Neural arches	na	Paired element forming an arch surrounding the neural canal on the dorsal side of a vertebra; develop from the basidorsal arcualia.
Neural spines	ns	Distal extensions of the neural arches dorsal to the neural canal. Neural spines are usually paired (nsp) but can also be median in the last few preural centra and ural centra.
Opisthural lobe	ol	Protruding fin-like structure, in which the notochord extends, emerging from the dorsal base of the caudal fin lobe and lying superior to it in young fish. Previously referred to as “notochordal appendage” (Carpenter, 1975).
Parapophyses	pp	Lateral or ventrolateral projections of vertebrae arising through replacement ossification of basiventrals or direct formation into bone.
Parhypural	phy	Haemal element supported by preural centrum 1 (pu1). The arch of the parhypural represents the exit point of the main caudal arteries and veins.
Plate of connective tissue	pct	Term generally used for teleosts; cartilaginous elements on the distal portion of some hypaxial elements; thought to support the caudal fin rays together with the distal radials; also described as “core of connective tissue”.
Polyural caudal skeleton		Type of caudal skeleton characterized by the presence of more than two ural centra.
Preural centrum	pu	Vertebral centrum of the caudal fin region preceding the ural centra, bearing both neural and haemal arches and usually both neural and haemal spines. A preural centrum does not support hypurals. Preural caudal centra are numbered from the posterior-most, which supports the parhypural, to the anterior-most.
Principal caudal rays		The segmented and branched dermoskeletal rods plus usually one unbranched but segmented rod located at each of the dorsal and ventral edges of the caudal fin; associated with endoskeletal elements.
Procurrent caudal ray		Dermoskeletal rods, shorter than a principal caudal ray, which form the dorsal and ventral series of lepidotrichia of median fins and are associated with endoskeletal elements, such as pterygiophores, neural and haemal spines, epurals, and uroneurals.
Proximal radials		Refers to haemal elements and hypurals in contrast to distal radials that are located distal to haemal elements and hypurals.
Pterygiophores	pt	Bones or cartilages, independent of the axial skeleton, that articulate with the base of the rays of the median fins (dorsal and anal fins); In polypteriformes, pterygiophores also support all the caudal dorsal lepidotrichia, even the most posterior ones which we include here in the caudal fin.
Supraneural	sn	Independent, median, elongated, rod-like cartilages or bones dorsal to the notochord and developing independently of the neural spines.
Ural centra	u	Posterior-most centra of the vertebral column characterized by the absence of haemal arches. Ural centra support hypurals ventrally and are numbered beginning from anterior to posterior (ural centrum 1, u1, supports hypural 1).
Uroneural	un	Modified neural arch elements, and consequently, paired, elongated bones that extend along the dorso-lateral surface of the last preural centra and/or ural centra and dorso-lateral to the notochord.
Urostyle	ust	Posterior region of the caudal fin axial endoskeleton of some teleosts; interpreted as the result of the fusion of preural centrum 1 (pu1) and a variable number of ural centra.
Vertebra		Includes one set of all serially repeated, ossified, cartilaginous, and ligamentous elements around the notochord, consisting of centrum, neural arch and spine, and haemal arch and spine.